HHS Public Access

Author manuscript

Psychiatry Res. Author manuscript; available in PMC 2016 September 30.

Altered threat and safety neural processing linked to persecutory delusions in schizophrenia: a two-task fMRI study

David L. Perez[a], **Hong Pan**[a,b], **Daniel S. Weisholtz**[a,c], **James C. Root**[d], **Oliver Tuescher**[e,f], **David B. Fischer**[a], **Tracy Butler**[g], **David R. Vago**[a], **Nancy Isenberg**[h], **Jane Epstein**[a], **Yulia Landa**[i], **Thomas E. Smith**[j], **Adam J. Savitz**[i], **David A. Silbersweig**[a,c], and **Emily Stern**[a,b,*]

[a]Functional Neuroimaging Laboratory, Brigham and Women's Hospital, Harvard Medical School, Department of Psychiatry, Chestnut Hill, MA, USA

[b]Brigham and Women's Hospital, Department of Radiology, Harvard Medical School, Boston, MA, USA

[c]Brigham and Women's Hospital, Department of Neurology, Boston, MA, USA

[d]Memorial Sloan Kettering Cancer Center, Department of Psychiatry and Behavioral Sciences, New York, NY, USA

[e]University Medical Center Freiburg, Department of Neurology, Freiburg im Breisgau, Germany

[f]University Medical Centre Mainz, Department of Psychiatry and Psychotherapy, Mainz, Germany

[g]Langone Medical Center, New York University School of Medicine, New York, NY, USA

[h]Neuroscience Institute, Virginia Mason Medical Center, Seattle, WA, USA

[i]Weill Cornell Medical Center, Department of Psychiatry, New York, NY, USA

[j]New York State Psychiatric Institute, Columbia University, New York, NY, USA

Abstract

Persecutory delusions are a clinically important symptom in schizophrenia associated with social avoidance and increased violence. Few studies have investigated the neurobiology of persecutory delusions, which is a prerequisite for developing novel treatments. The aim of this two-paradigm

*Corresponding author: Functional Neuroimaging Laboratory, Brigham and Women's Hospital/Harvard Medical School, 824 Boylston Street, Chestnut Hill, MA 02467, USA. Tel.: +1 617-732-9127; Fax: +1 617-732-9151. estern3@partners.org.

functional magnetic resonance imaging (fMRI) study is to characterize social "real world" and linguistic threat brain activations linked to persecutory delusions in schizophrenia (*n*=26) using instructed-fear/safety and emotional word paradigms. Instructed-fear/safety activations correlated to persecutory delusion severity demonstrated significant increased lateral orbitofrontal cortex and visual association cortex activations for the instructed-fear vs. safety and instructed-fear vs. baseline contrasts; decreased lateral orbitofrontal cortex and ventral occipital-temporal cortex activations were observed for the instructed-safety stimuli vs. baseline contrast. The salience network also showed divergent fear and safety cued activations correlated to persecutory delusions. Emotional word paradigm analyses showed positive correlations between persecutory delusion severity and left-lateralized linguistic and hippocampal-parahippocampal activations for the threat vs. neutral word contrast. Visual word form area activations correlated positively with persecutory delusions for both threat and neutral word vs. baseline contrasts. This study links persecutory delusions to enhanced neural processing of threatening stimuli and decreased processing of safety cues, and helps elucidate systems-level activations associated with persecutory delusions in schizophrenia.

Keywords

1. Introduction

Schizophrenia is characterized by prominent disturbances in social-emotional cognition, perception, executive function, behavior and self-awareness. Symptoms in schizophrenia have traditionally been segregated into positive, negative, cognitive, thought disorganization, psychomotor and mood components (Tandon et al., 2009). Positive symptoms include hallucinations and delusions, each defined in part by distortions in reality perception. While the neural basis of auditory hallucinations in schizophrenia has been extensively investigated (Silbersweig et al., 1995; Silbersweig and Stern, 1996; Epstein et al., 1999; Lennox et al., 2000; Raij et al., 2009; Jardri et al., 2011), the neurobiology of delusions has not been so well characterized. Delusions of persecution are among the most commonly reported fixed, false beliefs endorsed by patients with schizophrenia. Patients experiencing persecutory delusions exhibit heightened anticipation and recall of aversive events, increased social avoidance (Moutoussis et al., 2007), and salience misattributions (Kapur, 2003; Holt et al., 2006b). Patients with schizophrenia who have prominent paranoia also report unstable assessments of themselves and their environment (Melo et al., 2006). Epidemiologic studies in schizophrenia suggest a prevalence of 3-12% for serious violent behavior and a particular association between violent behavior and persecutory delusions (Swanson et al., 2006; Coid et al., 2013), underscoring the importance of better understanding this clinically-meaningful symptom. Furthermore, mistrust of mental health professionals is a commonly encountered barrier to treatment adherence, and a specific relationship between lack of treatment, persecutory delusions, and violence has been reported (Keers et al., 2014). Identifying the neurobiology underlying paranoia is therefore critical, and may pave the way for novel treatments.

Neuroimaging investigations of social-emotional processing in schizophrenia, to date, have largely used emotionally valenced face-viewing probes (Gur et al., 2002; Gur et al., 2007; Li et al., 2010; Taylor et al., 2012). Compared with healthy subjects, patients with schizophrenia demonstrated reduced activations in bilateral amygdala, parahippocampal gyri, fusiform gyri, right superior frontal gyrus, and lentiform nucleus during emotional face processing (Li et al., 2010). A meta-analysis of amygdalar activations across aversive stimuli in schizophrenia identified decreased amygdalar activations for negative versus neutral interaction contrasts. This effect, however, was partially explained by increased amygdalar activation to neutral stimuli in schizophrenic subjects (Holt et al., 2006a; Hall et al., 2008; Anticevic et al., 2012).

Few neuroimaging studies have investigated prefrontal, limbic/paralimbic and sensory processing abnormalities associated with social-emotional cognition in patients with schizophrenia who are currently experiencing paranoid delusions (Kay et al., 1987; Phillips et al., 1999; Williams et al., 2004; Russell et al., 2007; Williams et al., 2007; Pinkham et al., 2008). In a functional magnetic resonance imaging (fMRI) study of 10 patients with schizophrenia (5 paranoid, 5 non-paranoid) using an affectively valenced face-viewing paradigm, paranoid individuals exhibited increased activations in insular, fusiform, lingual cortices, and cerebellum compared to non-paranoid patients during fearful face processing (Phillips et al., 1999). In an fMRI study that segregated schizophrenic patients dichotomously as paranoid or non-paranoid based on the presence or absence of elevated scores in four positive symptom items of the Positive and Negative Syndrome Scale (PANSS) (Kay et al., 1987), paranoid compared to non-paranoid subjects showed increased right frontopolar cortex and decreased bilateral fusiform and lingual gyrus activations to fearful versus neutral faces (Williams et al., 2004). Furthermore, accounting for autonomic arousal, paranoid individuals exhibited reduced amygdalar activations. Additional studies have characterized reduced activations in the amygdala, hippocampus, anterior cingulate cortex (ACC), and insula in paranoid versus non-paranoid schizophrenia using affectively valenced facial viewing paradigms (Russell et al., 2007; Williams et al., 2007).

Social learning of fear (instructed-fear) paradigms allow individuals to obtain fear and safety information through explicit verbal communication, and offer promise in elucidating neural mechanisms associated with salience misattributions and abnormal social fear learning and expression in paranoid schizophrenia (Phelps et al., 2001; Olsson and Phelps, 2007). In classical, Pavlovian fear conditioning paradigms, by comparison, a neutral conditioned stimulus (CS+) is paired with a naturally aversive unconditioned stimulus (US); an implicitly learned fear association is invoked by the CS+ alone following repeated CS-US pairings (Rogan et al., 2005). A second control conditioned stimulus (CS-), not paired with the US, is often also included. Schizophrenic patients show associative learning deficits exemplified by heightened CS- related autonomic activity and impaired extinction learning(Holt et al., 2009). Functional MRI studies have found blunted left middle insula activation to US presentations (Linnman et al., 2013), increased ventral striatum activation to neutral (CS-) stimuli (Jensen et al., 2008), and reduced ventromedial prefrontal cortex (vmPFC) activation during extinction (Holt et al., 2012) in schizophrenic patients compared to healthy subjects. Impaired extinction and vmPFC hypoactivation was particularly noted in patients with delusions. Instructed-fear paradigms, in which subjects are explicitly instructed

as to the CS-US associations before the experiment but are not ever presented with the US during the task, approximate "real world" threat more closely than fear conditioning probes because the anticipation of threat is the primary cognitive state that is elicited. In healthy subjects, instructed-fear cues activate bilateral dorsal ACC, anterior insula, striatum, and right pallidum (Butler et al., 2005; Butler et al., 2007b; Mechias et al., 2010). In the only published study to date in psychotic populations using this paradigm, schizophrenic subjects with serious violence histories compared to schizophrenic individuals without prior violence demonstrated enhanced activations in right orbitofrontal cortex (OFC), left subgenual ACC, and bilateral temporo-occipital cortex for instructed-fear stimuli (Kumari et al., 2009).

In terms of emotional-linguistic function, evidence suggests impaired emotional word processing in schizophrenia. While studies have yielded some conflicting results(Pinheiro et al., 2012), schizophrenic patients have rated negatively valenced words more negatively and positively valenced words less positively compared to controls (Jalenques et al., 2013). A recall bias for negatively valenced words has also been observed in schizophrenia (Calev and Edelist, 1993). In a study comparing patients experiencing predominantly persecutory delusions compared to non-paranoid schizophrenic and healthy cohorts, delusional individuals more frequently classified words as unpleasant and demonstrated delayed classification of neutral words (Holt et al., 2006b). In an fMRI study using two-sentence, affectively valenced descriptors of social situations, schizophrenic patients showed increased posterior cingulate gyrus activations to neutral, relative to negative, sentence pairs (schizophrenic patients also showed increased medial prefrontal and posterior cingulate cortex activations to neutral, relative to positive, sentence pairs) (Holt et al., 2011). Healthy subjects exhibited an opposite pattern of activations, and delusion severity in this schizophrenia cohort correlated with cingulate gyri activations to neutral sentence pairs.

In this study, we used instructed-fear/safety and emotional word paradigms specifically relevant to patients with paranoid delusions to characterize correlations between the clinically salient dimension of persecutory delusions and neural activations in 26 patients with schizophrenia. This two-task approach enabled the investigation of convergent and stimuli/modality specific neural activations associated with persecutory delusion severity. Our laboratory has previously implemented instructed-fear/safety paradigms to probe frontolimbic and subcortical emotional processing in healthy subjects (Butler et al., 2005; Butler et al., 2007b) and anxiety disorders (Tuescher et al., 2011). Emotional word fMRI paradigms have also been designed by our group to investigate emotional-linguistic processing in healthy subjects (Isenberg et al., 1999; Protopopescu et al., 2005a) and neuropsychiatric populations (Protopopescu et al., 2005b; Epstein et al., 2006; Silbersweig et al., 2007; Epstein et al., 2011). The dimensional symptom-specific approach used in this study has been used previously by our laboratory to characterize brain-symptom relationships in other neuropsychiatric disorders (Protopopescu et al., 2005b). Applying instructed-fear/safety and emotional word fMRI paradigms, we hypothesized increased frontolimbic and modality-specific neural processing of threatening stimuli and decreased processing of safety cues. Specifically, we hypothesized increased amygdalar-hippocampal activations to threat, divergent salience network modulation by threat and safety cues, and increased ventral visual stream and language network activations to social and linguistic threat associated with persecutory delusion severity in patients with schizophrenia.

2. Methods

2.1. Subjects

Twenty-six, right-handed subjects (6 female, 20 male; mean age=29.85, range 20-44) participated in this study. Participants were diagnosed with schizophrenia (*n*=22) or schizoaffective disorder (*n*=4) based on the Structured Clinical Interview for the Diagnostic and Statistical Manual of Mental Disorders IV Axis I Disorders (First, 1997). All subjects were receiving antipsychotic medications [typical (*n*=4), atypical (*n*=18), typical and atypical (*n*=4), with antipsychotic doses converted to a mean daily dose equivalence of chlorpromazine for each subject (mean=553.19 mg, SD=270.69 mg) (Andreasen et al., 2010). Subjects were also taking the following psychotropic medications: mood stabilizers (8); antidepressants (6); benzodiazepines (5); anti-cholinergic medications (5). Inclusion criteria included the following: presence of only minimal negative symptoms and cognitive impairment, no history of electroconvulsive therapy within the past year, English as first language or fully fluent in English, and capacity to provide informed consent. Exclusion criteria included: a diagnosis of schizoaffective disorder with mainly affective symptoms, prior manic episode, substance abuse within the past six months, and a history of major medical and/or neurologic illness. Paranoid delusion severity was based on the persecution/suspiciousness item (P6) of the PANSS (Kay et al., 1987) (mean=2.96, SD=1.45, P6=1-2 (9), P6=3 (8), P6=4-6 (9)); higher scores indicated increased perceived persecution and suspicious hypervigilance. Complete PANSS scores were available for 23 of 26 subjects (PANSS total mean=51.17, SD=17.40; PANSS positive subscale mean=12.17, SD=4.92; PANSS negative subscale mean=13.91, SD=5.28; PANSS general subscale mean=25.09, SD=9.54). An analysis of covariance (ANCOVA) performed to evaluate associations between p6 score and PANSS total score with age, sex and mean daily dose equivalence of chlorpromazine entered as covariates was not statistically significant(p=0.0843). All subjects provided informed consent before enrollment, which was part of a protocol approved by the institutional review board of New York Presbyterian Hospital/Weill Cornell Medical College. Data analyses and manuscript preparation for this protocol were approved by the Partners Human Research Committee.

2.2. Instructed-fear/safety paradigm

2.2.1. Threshold setting procedure—As previously described (Butler et al., 2005; Butler et al., 2007b), immediately before scanning, participants determined the level of electrodermal stimulation to be received during the scan session via a dial-up procedure in which stimulations to the left wrist were increased gradually to a level of intensity experienced by that individual as "uncomfortable but not painful," with the aim of standardizing perceived stimulation aversiveness across subjects. Following the dial-up procedure, participants were told "all stimulations you receive during this study will be of exactly this strength and duration."

2.2.2. Experimental paradigm—The scanning session consisted of a "fear" condition, about which participants were told before the scanning session "an electrodermal stimulation can occur at any time" in conjunction with a specified colored square, and a "safety" condition for which participants were verbally instructed before the scanning session that

they would not receive any electrodermal stimulations associated with a distinct colored square. Fear and safety conditions were signified by the presentation of easily-distinguishable blue or yellow colored squares via a MR-compatible screen. Stimuli presentation was controlled by the Integrated Functional Imaging System (*In vivo*, Orlando, FL, USA) by means of E-Prime software (Psychology Software Tools, Pittsburgh, PA, USA). Pairing of colors with conditions was counterbalanced across participants. Each color appeared for 12 s followed by 18 s of rest (30-s condition period). There were five pseudo-randomly ordered periods of each color per scanning run (each run was preceded by a 20-s rest period), and two scanning runs per study session. No motor response was required. Participants did not actually receive any electrodermal stimulation during scanning.

2.3. Emotional word paradigm

In a second fMRI paradigm, participants read 48 printed words, 24 of which were selected for their threatening content and negative valence so as to be particularly relevant to individuals with paranoid delusions, e.g., "persecute," "threat," and "spy." The remaining 24 words were selected for their emotionally neutral content, e.g., "arrange," "rotate," and "folder." The two word categories were counterbalanced for the possible confounding variables of word length, frequency within the lexicon (Carroll et al., 1971), and part of speech. Subjects were instructed to read each word silently and then to immediately press a button under their right index finger. The stimuli were presented in a block design consisting of four blocks of six threat (T) words each and four blocks of six neutral (N) words each. The blocks were intermixed in a pseudorandom order (NTTNNTNT). Each word appeared for 2 s with an interstimulus interval jittered based on a uniform distribution on the range [1.8, 3.8] (average of 2.8 s), for a total of 28.8 s per block. Each block was followed by 24 s of rest, with the paradigm as a whole preceded and followed by two 12-s rest periods. During rest periods, subjects were instructed to look at a dash at the center of the screen. Immediately after imaging was completed, subjects were removed from the scanner and their memory for the specific stimuli seen in the scanner was tested with a list consisting of the 48 stimuli seen during scanning (targets) and 24 novel words (distractors) with which the targets were interspersed. Distractors were divided equally into threat and neutral words and balanced for the same qualities as the target words. The subjects were instructed to read each word and to indicate those words that they believed they had seen in the scanner. Following this task, subjects rated the emotional valence of each word on a seven-point Likert scale (-3=strongly negative, 0=neutral, +3=strongly positive).

The order of the instructed-fear/safety and emotional word paradigms was counterbalanced across subjects.

2.4. Image acquisition

Image data were acquired using exactly the same protocol on one of two research-dedicated General Electric-Signa 3 Tesla MRI scanners (max gradient strength 40 mT/m; max slew rate 150T/m/s; scanner 1: 11 participants; scanner 2: 15 participants). Since there were no detectable differences in imaging data acquired on the two scanners as confirmed via ANCOVA with the scanner ID as a covariate (independent variable) for inter-subject variation and blood-oxygen-level-dependent (BOLD) signal as the dependent variable,

datasets were combined. Following a standard T1 weighted localizer scan, a high-resolution T1 weighted anatomical image was acquired using a spoiled gradient recalled acquisition sequence [repetition time (TR)/echo time (TE)=30/8 ms, flip angle=45, field of view=220 mm, 140 coronal slices with thickness=contiguous 1.5 mm, number of averages=1, matrix=256×256, voxel resolution=0.8594×1.5×0.8594 mm^3]. Echo planar imaging (EPI) was used to obtain BOLD functional MR images. After shimming to maximize homogeneity, a series of gradient echo fMRI scans were acquired (TR=1200 ms, TE=30 ms, flip angle=70, field of view=240 mm, 15 or 21 slices, slice thickness=5 mm, interslice gap=1 mm, matrix=64×64, voxel resolution=3.75×3.75×6 mm^3) with a z-shimming algorithm to reduce susceptibility artifact at the base of the brain (Gu et al., 2002). A reference T1-weighted anatomical image with the same slice placement and thickness and a matrix of 256×256 was acquired immediately before the EPI acquisition.

2.5. Image processing and analysis

Data processing with a customized Statistical Parametric Mapping (SPM) software package (Wellcome Department of Imaging Neuroscience, University College, London, UK; (www.fil.ion.ucl.ac.uk/spm)) consisted of: reconstruction of echoplanar functional images using modified GE reconstruction software; manual anterior commissure-posterior commissure re-orientation of all anatomical and EPI images; realignment to correct for slight head movement between scans based on intracranial voxels (data sets with head movement of greater than 1/3 voxel over the study session were excluded); extraction of physiological fluctuations such as cardiac and respiratory cycles from EPI image sequences (Frank et al., 2001); co-registration of functional EPI images to the corresponding high-resolution anatomical image based on the rigid body transformation parameters of the reference anatomical image to the latter for each individual subject; stereotactic normalization to a standardized coordinate space (Montreal MRI Atlas version of Talairach space with the Montreal Neurological Institute [MNI] average of 152 T1 brain scans) based on the high-resolution anatomical image to normalize for individual differences in brain morphology; and spatial smoothing with an isotropic Gaussian kernel (full width at half-maximum=7.5 mm) to increase signal-to-noise ratio.

For image data analyses, a two-level voxel-wise linear fixed-effects model was constructed using customized fmristat software in an ANCOVA setting (Worsley et al., 2002). First, at the individual subject level, a whole-brain voxel-wise multiple linear regression model was employed. This was composed of the regressor of interest, which consisted of the stimulus onset times convolved with a prototypical hemodynamic response function, and the covariates of no-interest, which included the temporal first order derivative of the principal regressors (to compensate for slight latency differences in individual hemodynamic response from the prototypical response function), global fluctuations, physiological fluctuations, realignment parameters, and scanning periods. Temporal filtering was performed to counter the effects of baseline shifts and higher frequency noise (than prototypical hemodynamic response), and a first order autoregressive (1) model of the time course was used to accommodate temporal correlation in consecutive scans. Effects at every brain voxel were estimated using the expectation maximization algorithm, and regionally specific effects were then compared using linear contrasts. That is, for each subject, the effect image and its

standard error image for each condition were calculated, and these were also combined in a series of linear contrasts entered into the second stage group-level correlation analysis. At the group level, the within-group effects of the hypothesis-driven contrasts were examined for their association with the P6 item score via a multiple regression model, with the P6 score as the main regressor, and age, sex, and mean daily dose equivalent of chlorpromazine as covariates of no-interest. For the instructed-fear/safety data, only planned contrasts were examined: (1) instructed-fear vs. safety; (2) instructed-fear vs. baseline; and (3) instructed-safety vs. baseline. For the emotional word data, only planned contrasts were examined: (A) threat vs. neutral words; (B) threat words vs. baseline; and (C) neutral words vs. baseline. These group-level correlation effect estimates generated statistical maps of the t-statistic, and the statistical significance of the t-maps was then evaluated in the final step of inference. The statistical inference is based on random field theory as implemented in fmristat, where the t-statistical maps were thresholded initially at a voxel-wise two-tailed p-value < 0.01 (based on which cluster sizes of activated/deactivated areas were reported), and the group-level correlation effect of interest at a peak coordinate was considered significant if the corrected p-value < 0.05, which was based on family-wise error rate correction of the voxel-wise p-values over the entire brain. Peak coordinates and sub-maxima were specifically reviewed for inclusion of the left human color area (V4) (x: -20 to -38; y: -70 to -90; z: -8 to -15; MNI coordinates) (McKeefry and Zeki, 1997) in the instructed-fear/safety contrasts and at the visual word form area (VWFA) (x: -42±5; y: -58±8; z: -17±6; MNI coordinates) (Cohen et al., 2000; McCandliss et al., 2003; Glezer and Riesenhuber, 2013) in the emotional word contrasts.

Post-scan behavioral test data recognition rates and valence ratings were analyzed using repeated-measures ANCOVA. Recognition memory performance was assessed by calculating a discrimination index d' per word valence type for each individual based on Signal Detection Theory, estimated by the z score of the false alarm rate minus the z score of the hit rate. Also, for the behavioral data analysis, subjects were stratified into 3 subgroups of non-paranoid (P6 score: 1-2), mildly paranoid (P6 score: 3), and paranoid (P6 score: 4-6) for statistical testing of persecutory delusion severity as a group factor. Age, sex and mean daily dose equivalence of chlorpromazine were entered as covariates of no-interest.

3. Results

3.1. Behavioral results

3.1.1. Recognition memory—There was a statistically significant main effect of word valence type in recognition rate ($F(1,34)=5.48$, $p=0.025$) where d' (Threat) $> d'$ (Neutral). This difference was most pronounced for the non-paranoid group (P6 score: 1-2) and less so for the mildly paranoid (P6 score: 3) and paranoid (P6 score: 4-6) groups. There was no significant effect of group, age or mean daily dose equivalence of chlorpromazine in recognition rates, though there was a mild effect of sex ($F(1,34)=4.23$, $p=0.047$).

3.1.2. Valence ratings—There was a statistically significant main effect of group ($F(2,60)=6.21$, $p=0.004$), word valence type ($F(1,60)=289.73$, $p<0.0001$), and group by valence type interaction ($F(2,60)=5.83$, $p=0.0049$) in valence rating. Valence rating

differences between threat and neutral words were most pronounced in the non-paranoid group (P6 score: 1-2), less in the mildly paranoid group (P6 score: 3), and least in the paranoid group (P6 score: 4-6). There was no significant effect of age, sex or mean daily dose equivalence of chlorpromazine in valence rating.

3.2 Instructed-fear/safety neuroimaging results

Analyses were performed on 22 subjects (18 male, 4 female; mean age=28.13, range 20-43; mean P6 score=2.78, SD=1.48, P6=1-2 (9), P6=3 (7), P6=4-6 (6); 2 of 26 total subjects either refused to participate or aborted the task due to anxiety; 2 of 26 participants were excluded following data quality control evaluations).

To assess the correlation between P6 scores and BOLD activations the following contrasts were calculated: (1) instructed-fear vs. safety; (2) instructed-fear vs. baseline; and (3) instructed-safety vs. baseline (Table 1, Fig. 1, and Fig. 2). With the contrast instructed-fear vs. safety, P6 scores correlated positively with activations in visual processing areas (bilateral calcarine cortices, lingual gyri (including left V4 color area), left fusiform gyrus), bilateral lateral OFC/inferior frontal gyri, and left frontopolar cortex. P6 scores correlated negatively with activations in paralimbic areas (bilateral posterior-dorsal ACC, right insula) and default mode network (DMN) regions (right precuneus, supramarginal, angular gyri). For instructed-fear vs. baseline, P6 scores correlated positively with activations in visual processing regions (bilateral calcarine, lingual and fusiform cortices), lateral OFC/inferior frontal gyri, and right anterior hippocampus. P6 scores correlated negatively with activations in paralimbic regions (right posterior-dorsal ACC, middle insula, left rostral ACC), visual processing regions (bilateral middle/inferior occipital, left lingual, right cuneus gyri), and DMN regions (right posterior cingulate cortex/precuneus, left angular gyrus). For instructed-safety vs. baseline, P6 scores correlated positively with activations in visual processing regions (bilateral calcarine, fusiform, superior occipital cortices, right middle occipital, lingual gyri) and paralimbic areas (bilateral dorsal ACC, anterior insula). P6 scores correlated negatively with activations in visual processing regions (bilateral calcarine, lingual (including left V4 color area), inferior occipital gyri, right cuneus, left middle occipital, fusiform gyri) and limbic/paralimbic areas (bilateral lateral OFC/inferior frontal gyrus, right ventral striatum).

3.3. Emotional word paradigm neuroimaging results

Analyses were performed on 23 subjects (19 male, 4 female; mean age=30.22, range 20-44; mean P6 score=3.05, SD=1.42, P6=1-2 (7), P6=3 (7), P6=4-6 (9); 2 of 26 total subjects did not participate due to technical scanner-paradigm delivery issues, 1 of 26 participants was excluded following data quality control evaluations) to assess the correlation between P6 scores and BOLD activations during (1) threat words vs. neutral words; (2) threat words vs. baseline; (3) neutral words vs. baseline (Table 2, Fig. 3 and Fig. 4). With the contrast threat vs. neutral words, P6 scores correlated positively with activations in semantic processing regions (left lateralized inferior frontal, superior temporal gyri), limbic/paralimbic areas (bilateral vmPFC, left insula, parahippocampus, hippocampus, amygdala (trend)), and bilateral frontopolar cortices. P6 scores correlated negatively with activations in visual processing regions (left calcarine, cuneus), semantic processing regions (bilateral superior/

middle temporal gyri, right inferior frontal gyrus), and the right inferior parietal lobule (angular/supramarginal gyri). For threat words vs. baseline, P6 scores correlated positively with activations in visual ventral stream areas (bilateral middle occipital, cuneus, inferior temporal and fusiform gyri (VWFA), left calcarine, superior/middle occipital, right lingual gyri), semantic processing regions (left > right inferior frontal gyrus, bilateral superior/middle temporal gyri, opercular rolandic), and limbic/paralimbic areas (bilateral anterior-dorsal ACC, OFC, parahippocampal gyri, insula, left amygdala (trend)). P6 scores correlated negatively with activations in visual processing areas (bilateral calcarine, cuneus, right lingual and fusiform gyri), paralimbic regions (right rostral ACC, subgenual ACC, and OFC), DMN regions (bilateral angular gyri, precuneus, right temporoparietal junction/supramarginal and left posterior cingulate cortex), and bilateral frontopolar cortex. For neutral words vs. baseline, P6 scores correlated positively with activations in ventral visual stream processing areas (bilateral calcarine, superior occipital cortices, lingual, middle occipital, inferior temporal, fusiform gyri (VWFA), left inferior occipital gyrus), semantic processing regions (bilateral inferior frontal, superior/middle temporal gyri, left opercular rolandic), and paralimbic regions (bilateral anterior insula, right anterior-dorsal ACC, left mid-OFC). P6 scores correlated negatively with activations in visual processing areas (bilateral calcarine cortices, left cuneus, middle occipital, fusiform gyri, right inferior occipital and lingual gyri), limbic/paralimbic regions (bilateral posterior-medial OFC, vmPFC, parahippocampus, and left hippocampus), semantic processing regions (bilateral inferior frontal gyri, left middle temporal), bilateral frontopolar cortices, precuneus and left angular gyrus.

4. Discussion

This two-paradigm fMRI study probed the neurocircuitry of persecutory (paranoid) delusions in schizophrenia using complementary social-emotional-linguistic paradigms: an instructed-fear/safety (anticipatory threat) task and an emotional word (linguistic threat) paradigm comprised of threatening, negatively valenced words particularly relevant to individuals experiencing paranoid delusions.

4.1. Enhanced fear and decreased safety related sensory processing associated with persecutory delusion severity

In response to instructed-fear/safety stimuli that were differentiated from one another by distinct colored squares, patients demonstrated prominent modulation of visual processing and limbic/paralimbic regions correlated with persecutory delusion severity (P6 scores). For the instructed-fear vs. safety contrast, patients exhibited increased activations in primary and association visual cortices and lateral OFC. While similar activations were noted for instructed-fear stimuli correlated to P6, instructed-safety cues increased primary visual cortex activations and decreased lateral OFC and ventral occipital-temporal (including V4 color area) activations.

The pattern of fear- and safety-mediated lateral OFC activations can be contextualized using the neuroanatomical studies of Ongur, Price and colleagues (Ongur and Price, 2000; Ongur et al., 2003; Price and Drevets, 2010) and neurobiological investigations of learned safety.

The orbital prefrontal network, which consists of the posterior central and lateral OFC including the pars orbitalis portion of the inferior frontal gyrus (Brodmann area 47), receives afferents from sensory cortices including visual processing regions (Rolls and Baylis, 1994). In the context of multi-modal sensory integration, the lateral OFC is implicated in behavioral choice selection for perceived rewards (Elliott et al., 2000). The association of increased persecutory delusion severity correlated with increased lateral OFC and left V4 color area activations for instructed-fear cues, and an inverse pattern of decreased lateral OFC and left V4 color area activations with instructed-safety cues, suggests enhanced higher-order sensory processing of threat and diminished processing of safety signals for behavioral choice selection. This is further supported by the finding of a negative correlation between right ventral striatum activation and persecutory delusion severity during processing of instructed-safety cues. Safety signals have been linked to increased exploratory behaviors, reward, anti-depressant like-properties, and potentiated striatal activity in animal models of learned safety (Rogan et al., 2005; Pollak et al., 2008). Given that paranoid delusions are associated with increased social avoidance(Moutoussis et al., 2007), it can be theorized that increased sensory processing of potentially threatening stimuli and decreased processing of safety signals may mediate aspects of restrictive, hypervigilant social behaviors in patients experiencing persecutory delusions.

4.2. Divergent fear and safety associated salience network activations

For the instructed-fear vs. safety contrast, patients also showed decreased activations in bilateral posterior-dorsal ACC and right insula correlated with delusion severity. Conversely, when viewing instructed-safety cues delusion severity positively correlated with bilateral dorsal ACC and anterior insula activations and negatively correlated with right ventral striatum activation. These findings are noteworthy given that delusional misattributions in psychosis have been linked to aberrant salience processing in schizophrenia (Kapur, 2003). In addition to the ventral striatum (Taylor et al., 2005; Juckel et al., 2006; Jensen et al., 2008), the ACC and the insula are critical nodes in the large-scale salience network implicated in the pathophysiology of delusions (Palaniyappan and Liddle, 2012). Instructed-fear stimuli activate bilateral dorsal ACC and anterior insula in healthy subjects (Mechias et al., 2010), while currently paranoid compared to non-paranoid schizophrenic subjects have exhibited decreased ACC and insula activations in response to aversive face-viewing probes (Williams et al., 2007). As evident from the neural activations correlated to P6 scores in our cohort, instructed-fear cues reduced ACC-anterior insula activations while instructed-safety cues increased activations in these regions. This suggests that, as persecutory paranoid delusions worsened, increased ACC-insula recruitment for safety cues potentially reflected (particularly within the dorsal ACC) the degree of emotional conflict occurring as a consequence of the incongruence between safety signal delivery and a heightened state of perceived persecution (Egner et al., 2008).

4.3. Increased language network and VWFA activations for negative and neutral words

The emotional word paradigm induced robust semantic processing activations, particularly in the left inferior frontal gyrus for the threat vs. neutral word contrast. Interestingly, neutral word processing vs. baseline correlated to P6 scores recruited bilateral (right > left) inferior frontal gyri activations. In healthy subjects, the pars orbitalis (Brodmann area 47) of the

inferior frontal gyrus has been linked to controlled retrieval of semantic information, while the pars triangularis (Brodmann area 45) has been linked to post-retrieval verbal response selection (Badre and Wagner, 2007). Studies of language lateralization in schizophrenia (including paranoid schizophrenia) have identified bilateral cortical activations during linguistic tasks driven primarily by enhanced right hemisphere activations (Sommer et al., 2003; Li et al., 2007). Increased bilateral anterior language network activations to neutral words may mediate enhanced (dysfunctional) retrieval and processing of semantic information and potentially accounts for the previously characterized neutral word classification delay seen in patients with persecutory delusions (Holt et al., 2006b).

In response to emotionally valenced words, subjects also showed modulation of ventral visual stream and limbic/paralimbic regions correlated with persecutory delusion severity. As P6 scores increased, threat and neutral valence words each increased ventral visual stream activations in lingual, inferior temporal and fusiform gyri. In healthy subjects, linguistic threat has been shown to modulate limbic/paralimbic (e.g., amygdala, parahippocampus, medial OFC, ACC), semantic processing (vlPFC), and lingual gyrus activations (Isenberg et al., 1999; Lewis et al., 2007; Citron, 2012); negatively valenced pictures commonly increase occipital-temporal ventral visual stream ("what" pathway) activations (Taylor et al., 2000; Sabatinelli et al., 2005; Sabatinelli et al., 2009). Visual processing deficits in schizophrenia have increasingly been characterized as involving predominantly dorsal stream ("where" pathway) abnormalities (Butler et al., 2001; Braus et al., 2002; Chen et al., 2004; Butler et al., 2007a; Seymour et al., 2013). However, increased ventral stream activations were found in paranoid schizophrenic patients compared to healthy subjects during performance of a dual working memory, affectively valenced face-viewing task (Wolf et al., 2011). The ventral visual stream is implicated in object and face perception (Kanwisher and Yovel, 2006), and the left middle portion of the fusiform gyrus (VWFA) is specifically attuned for reading (although not exclusively) (Cohen et al., 2000; Dehaene and Cohen, 2011). Our cohort exhibited increased VWFA (McCandliss et al., 2003) activation in the threat word and neutral word vs. baseline contrasts. These results suggest a potential modality-specific threat (and neutral) bias for visual word and color (instructed-fear) perceptual processing associated with persecutory delusion severity in schizophrenia.

4.4. Increased threat related medial temporal activations

Medial temporal structures, including the parahippocampus, hippocampus, and amygdala, have been implicated in the pathophysiology of primary and secondary psychotic syndromes (Epstein et al., 1999; Butler et al., 2012). Our cohort demonstrated left lateralized parahippocampal, hippocampal, and amygdala (trend) activations correlated to P6 scores in the threat vs. neutral contrast in the emotional word paradigm, along with reduced left hippocampal and parahippocampal activations to neutral words. Instructed-fear stimuli correlated to P6 scores also exhibited increased right anterior hippocampal activation. These convergent findings suggest that as persecutory delusions worsened, negatively valenced stimuli increased medial temporal lobe activations, and linguistic threat was particularly associated with left-lateralized activations. Earlier studies in schizophrenia have reported impaired hippocampal habituation to fearful faces (Holt et al., 2005), a correlation between

left parahippocampal activations and positive psychotic symptoms in a self-other affectively valenced evaluative task (Pauly et al., 2013), and altered hippocampal-parahippocampal resting state functional connectivity (Zhou et al., 2008). Heightened hippocampal-parahippocampal and amygdalar activations to negatively valenced social-emotional-linguistic probes potentially link aberrant emotional memory retrieval, contextual fear, and salience processing to the neurobiology of persecutory delusions.

4.5. Synthesis, limitations and conclusions

Given this two-paradigm approach that probes social emotional and linguistic aspects of fear and safety processing, it is important to contextualize the findings using emotional processing/regulation models(Ochsner and Gross, 2005; Phillips et al., 2008; Etkin et al., 2011). Instructed-fear vs. safety stimuli correlated to persecutory delusion severity demonstrated increased threat and decreased safety evaluation (lateral OFC, ventral striatum) and over-appraisal of safety cues (dorsal ACC/dorsomedial prefrontal cortex). Linguistic threat activated lateral cognitive control regions (vlPFC), as well as regions implicated in automatic emotional processing/regulation (vmPFC, parahippocampus-hippocampus, amygdala). Anterior hippocampal activation was also associated with instructed-fear cues. Both instructed-fear and linguistic threat also shared enhanced reactivity in primary/secondary and associative sensory areas (V4, VWFA) suggestive of selective heightened perceptual processing in individuals with persecutory delusions.

There are several limitations in this study. Our cohort was on multiple psychotropic medications which were only partially controlled for by including mean daily dose equivalent of chlorpromazine as a covariate of no-interest in the analyses. In addition, while this study investigated neurocircuits linked to persecutory delusions, the findings are relative activation increases and decreases. The lack of a healthy control group could be seen as a limitation, however, this addition would not aid the study of persecutory delusion severity as a continuous variable. Also, while this study investigated a symptom complex (persecutory delusions) within patients diagnosed with a primary psychotic disorder, we cannot fully exclude that the neural associations identified may relate in part to other factors that potentially co-vary with persecutory delusions such as overall disease severity (although p6 scores were not predicted by PANSS total score in an ANCOVA). Future larger sample size analyses that control for additional potential confounds may provide added clarity. Lastly, activations in other regions implicated in cognitive-affective-linguistic-self referential processes (temporal pole(Pascual et al., 2015), DMN, cerebellum (Schmahmann and Sherman, 1998), thalamus) and arousal (brainstem) that correlated with P6 scores require further investigation.

In conclusion, this study linked enhanced neural processing of threatening (and neutral) stimuli and aberrant processing of safety cues in limbic-paralimbic and visual association regions to persecutory delusions in schizophrenia. Linguistic threat notably increased left-lateralized activations in anterior language areas and medial temporal lobe structures; neutral linguistic stimuli increased bilateral anterior language network activations. These data help elucidate systems-level biological mechanisms underlying persecutory delusions in schizophrenia.

Acknowledgments

References

Andreasen NC, Pressler M, Nopoulos P, Miller D, Ho BC. Antipsychotic dose equivalents and dose-years: a standardized method for comparing exposure to different drugs. Biological Psychiatry. 2010; 67:255–262. [PubMed: 19897178]

Anticevic A, Van Snellenberg JX, Cohen RE, Repovs G, Dowd EC, Barch DM. Amygdala recruitment in schizophrenia in response to aversive emotional material: a meta-analysis of neuroimaging studies. Schizophrenia Bulletin. 2012; 38:608–621. [PubMed: 21123853]

Badre D, Wagner AD. Left ventrolateral prefrontal cortex and the cognitive control of memory. Neuropsychologia. 2007; 45:2883–2901. [PubMed: 17675110]

Braus DF, Weber-Fahr W, Tost H, Ruf M, Henn FA. Sensory information processing in neuroleptic-naive first-episode schizophrenic patients: a functional magnetic resonance imaging study. Archives of General Psychiatry. 2002; 59:696–701. [PubMed: 12150645]

Butler PD, Martinez A, Foxe JJ, Kim D, Zemon V, Silipo G, Mahoney J, Shpaner M, Jalbrzikowski M, Javitt DC. Subcortical visual dysfunction in schizophrenia drives secondary cortical impairments. Brain. 2007a; 130:417–430. [PubMed: 16984902]

Butler PD, Schechter I, Zemon V, Schwartz SG, Greenstein VC, Gordon J, Schroeder CE, Javitt DC. Dysfunction of early-stage visual processing in schizophrenia. American Journal of Psychiatry. 2001; 158:1126–1133. [PubMed: 11431235]

Butler T, Pan H, Epstein J, Protopopescu X, Tuescher O, Goldstein M, Cloitre M, Yang Y, Phelps E, Gorman J, Ledoux J, Stern E, Silbersweig D. Fear-related activity in subgenual anterior cingulate differs between men and women. Neuroreport. 2005; 16:1233–1236. [PubMed: 16012355]

Butler T, Pan H, Tuescher O, Engelien A, Goldstein M, Epstein J, Weisholtz D, Root JC, Protopopescu X, Cunningham-Bussel AC, Chang L, Xie XH, Chen Q, Phelps EA, Ledoux JE, Stern E, Silbersweig DA. Human fear-related motor neurocircuitry. Neuroscience. 2007b; 150:1–7. [PubMed: 17980493]

Butler T, Weisholtz D, Isenberg N, Harding E, Epstein J, Stern E, Silbersweig D. Neuroimaging of frontal-limbic dysfunction in schizophrenia and epilepsy-related psychosis: toward a convergent neurobiology. Epilepsy & Behavior. 2012; 23:113–122. [PubMed: 22209327]

Calev A, Edelist S. Affect and memory in schizophrenia: negative emotion words are forgotten less rapidly than other words by long-hospitalized schizophrenics. Psychopathology. 1993; 26:229–235. [PubMed: 8190841]

Carroll, JB.; Davies, P.; Richman, B. The American Heritage Word Frequency Book. Houghton Mifflin Company; Boston, MA: 1971.

Chen Y, Levy DL, Sheremata S, Holzman PS. Compromised late-stage motion processing in schizophrenia. Biological Psychiatry. 2004; 55:834–841. [PubMed: 15050865]

Citron FM. Neural correlates of written emotion word processing: a review of recent electrophysiological and hemodynamic neuroimaging studies. Brain and Language. 2012; 122:211–226. [PubMed: 22277309]

Cohen L, Dehaene S, Naccache L, Lehericy S, Dehaene-Lambertz G, Henaff MA, Michel F. The visual word form area: spatial and temporal characterization of an initial stage of reading in normal subjects and posterior split-brain patients. Brain. 2000; 123(Pt 2):291–307. [PubMed: 10648437]

Coid JW, Ullrich S, Kallis C, Keers R, Barker D, Cowden F, Stamps R. The relationship between delusions and violence: findings from the East London first episode psychosis study. The Journal of the American Medical Association Psychiatry. 2013; 70:465–471. [PubMed: 23467760]

Dehaene S, Cohen L. The unique role of the visual word form area in reading. Trends in Cognitive Sciences. 2011; 15:254–262. [PubMed: 21592844]

Egner T, Etkin A, Gale S, Hirsch J. Dissociable neural systems resolve conflict from emotional versus nonemotional distracters. Cerebral Cortex. 2008; 18:1475–1484. [PubMed: 17940084]

Elliott R, Dolan RJ, Frith CD. Dissociable functions in the medial and lateral orbitofrontal cortex: evidence from human neuroimaging studies. Cerebral Cortex. 2000; 10:308–317. [PubMed: 10731225]

Epstein J, Pan H, Kocsis JH, Yang Y, Butler T, Chusid J, Hochberg H, Murrough J, Strohmayer E, Stern E, Silbersweig DA. Lack of ventral striatal response to positive stimuli in depressed versus normal subjects. American Journal of Psychiatry. 2006; 163:1784–1790. [PubMed: 17012690]

Epstein J, Perez DL, Ervin K, Pan H, Kocsis JH, Butler T, Stern E, Silbersweig DA. Failure to segregate emotional processing from cognitive and sensorimotor processing in major depression. Psychiatry Research: Neuroimaging. 2011; 193:144–150. [PubMed: 21764265]

Epstein J, Stern E, Silbersweig D. Mesolimbic activity associated with psychosis in schizophrenia. Symptom-specific PET studies. Annals of the New York Academy of Sciences. 1999; 877:562–574. [PubMed: 10415671]

Etkin A, Egner T, Kalisch R. Emotional processing in anterior cingulate and medial prefrontal cortex. Trends in Cognitive Sciences. 2011; 15:85–93. [PubMed: 21167765]

First, MB.; S, R.; Gibbon, M.; Williams, JBW. Structured Clinical Interview for DSM-IV (SCID). American Psychiatric Press; Washington, D.C.: 1997.

Frank LR, Buxton RB, Wong EC. Estimation of respiration-induced noise fluctuations from undersampled multislice fMRI data. Magnetic Resonance in Medicine. 2001; 45:635–644. [PubMed: 11283992]

Glezer LS, Riesenhuber M. Individual variability in location impacts orthographic selectivity in the "visual word form area". Journal of Neuroscience. 2013; 33:11221–11226. [PubMed: 23825425]

Gu H, Feng H, Zhan W, Xu S, Silbersweig DA, Stern E, Yang Y. Single-shot interleaved z-shim EPI with optimized compensation for signal losses due to susceptibility-induced field inhomogeneity at 3 T. Neuroimage. 2002; 17:1358–1364. [PubMed: 12414275]

Gur RE, Loughead J, Kohler CG, Elliott MA, Lesko K, Ruparel K, Wolf DH, Bilker WB, Gur RC. Limbic activation associated with misidentification of fearful faces and flat affect in schizophrenia. Archives of General Psychiatry. 2007; 64:1356–1366. [PubMed: 18056543]

Gur RE, McGrath C, Chan RM, Schroeder L, Turner T, Turetsky BI, Kohler C, Alsop D, Maldjian J, Ragland JD, Gur RC. An fMRI study of facial emotion processing in patients with schizophrenia. American Journal of Psychiatry. 2002; 159:1992–1999. [PubMed: 12450947]

Hall J, Whalley HC, McKirdy JW, Romaniuk L, McGonigle D, McIntosh AM, Baig BJ, Gountouna VE, Job DE, Donaldson DI, Sprengelmeyer R, Young AW, Johnstone EC, Lawrie SM. Overactivation of fear systems to neutral faces in schizophrenia. Biological Psychiatry. 2008; 64:70–73. [PubMed: 18295746]

Holt DJ, Coombs G, Zeidan MA, Goff DC, Milad MR. Failure of neural responses to safety cues in schizophrenia. Archives of General Psychiatry. 2012; 69:893–903. [PubMed: 22945619]

Holt DJ, Kunkel L, Weiss AP, Goff DC, Wright CI, Shin LM, Rauch SL, Hootnick J, Heckers S. Increased medial temporal lobe activation during the passive viewing of emotional and neutral facial expressions in schizophrenia. Schizophrenia Reseasrch. 2006a; 82:153–162.

Holt DJ, Lakshmanan B, Freudenreich O, Goff DC, Rauch SL, Kuperberg GR. Dysfunction of a cortical midline network during emotional appraisals in schizophrenia. Schizophrenia Bulletin. 2011; 37:164–176. [PubMed: 19605517]

Holt DJ, Lebron-Milad K, Milad MR, Rauch SL, Pitman RK, Orr SP, Cassidy BS, Walsh JP, Goff DC. Extinction memory is impaired in schizophrenia. Biological Psychiatry. 2009; 65:455–463. [PubMed: 18986648]

Holt DJ, Titone D, Long LS, Goff DC, Cather C, Rauch SL, Judge A, Kuperberg GR. The misattribution of salience in delusional patients with schizophrenia. Schizophrenia Research. 2006b; 83:247–256. [PubMed: 16540291]

Holt DJ, Weiss AP, Rauch SL, Wright CI, Zalesak M, Goff DC, Ditman T, Welsh RC, Heckers S. Sustained activation of the hippocampus in response to fearful faces in schizophrenia. Biological Psychiatry. 2005; 57:1011–1019. [PubMed: 15860342]

Isenberg N, Silbersweig D, Engelien A, Emmerich S, Malavade K, Beattie B, Leon AC, Stern E. Linguistic threat activates the human amygdala. Proceedings of the National Academy of Sciences of the United States of America. 1999; 96:10456–10459. [PubMed: 10468630]

Jalenques I, Enjolras J, Izaute M. Emotional valence of words in schizophrenia. Encephale. 2013; 39:189–197. [PubMed: 23199657]

Jardri R, Pouchet A, Pins D, Thomas P. Cortical activations during auditory verbal hallucinations in schizophrenia: a coordinate-based meta-analysis. American Journal of Psychiatry. 2011; 168:73–81. [PubMed: 20952459]

Jensen J, Willeit M, Zipursky RB, Savina I, Smith AJ, Menon M, Crawley AP, Kapur S. The formation of abnormal associations in schizophrenia: neural and behavioral evidence. Neuropsychopharmacology. 2008; 33:473–479. [PubMed: 17473838]

Juckel G, Schlagenhauf F, Koslowski M, Wustenberg T, Villringer A, Knutson B, Wrase J, Heinz A. Dysfunction of ventral striatal reward prediction in schizophrenia. Neuroimage. 2006; 29:409–416. [PubMed: 16139525]

Kanwisher N, Yovel G. The fusiform face area: a cortical region specialized for the perception of faces. Philosophical Transactions of the Royal Society of London. Series B, Biological Sciences. 2006; 361:2109–2128. [PubMed: 17118927]

Kapur S. Psychosis as a state of aberrant salience: a framework linking biology, phenomenology, and pharmacology in schizophrenia. American Journal of Psychiatry. 2003; 160:13–23. [PubMed: 12505794]

Kay SR, Fiszbein A, Opler LA. The Positive and Negative Syndrome Scale (PANSS) for schizophrenia. Schizophrenia Bulletin. 1987; 13:261–276. [PubMed: 3616518]

Keers R, Ullrich S, Destavola BL, Coid JW. Association of violence with emergence of persecutory delusions in untreated schizophrenia. American Journal of Psychiatry. 2014; 171:332–339. [PubMed: 24220644]

Kumari V, Das M, Taylor PJ, Barkataki I, Andrew C, Sumich A, Williams SC, Ffytche DH. Neural and behavioural responses to threat in men with a history of serious violence and schizophrenia or antisocial personality disorder. Schizophrenia Research. 2009; 110:47–58. [PubMed: 19230621]

Lennox BR, Park SB, Medley I, Morris PG, Jones PB. The functional anatomy of auditory hallucinations in schizophrenia. Psychiatry Research: Neuroimaging. 2000; 100:13–20. [PubMed: 11090721]

Lewis PA, Critchley HD, Rotshtein P, Dolan RJ. Neural correlates of processing valence and arousal in affective words. Cerebral Cortex. 2007; 17:742–748. [PubMed: 16699082]

Li H, Chan RC, McAlonan GM, Gong QY. Facial emotion processing in schizophrenia: a meta-analysis of functional neuroimaging data. Schizophrenia Bulletin. 2010; 36:1029–1039. [PubMed: 19336391]

Li X, Branch CA, Ardekani BA, Bertisch H, Hicks C, DeLisi LE. fMRI study of language activation in schizophrenia, schizoaffective disorder and in individuals genetically at high risk. Schizophrenia Research. 2007; 96:14–24. [PubMed: 17719745]

Linnman C, Coombs G 3rd, Goff DC, Holt DJ. Lack of insula reactivity to aversive stimuli in schizophrenia. Schizophrenia Research. 2013; 143:150–157. [PubMed: 23201307]

McCandliss BD, Cohen L, Dehaene S. The visual word form area: expertise for reading in the fusiform gyrus. Trends in Cognitive Sciences. 2003; 7:293–299. [PubMed: 12860187]

McKeefry DJ, Zeki S. The position and topography of the human colour centre as revealed by functional magnetic resonance imaging. Brain. 1997; 120(Pt 12):2229–2242. [PubMed: 9448578]

Mechias ML, Etkin A, Kalisch R. A meta-analysis of instructed fear studies: implications for conscious appraisal of threat. Neuroimage. 2010; 49:1760–1768. [PubMed: 19786103]

Melo SS, Taylor JL, Bentall RP. 'Poor me' versus 'bad me' paranoia and the instability of persecutory ideation. Psychology and Psychotherapy: Theory, Research and Practice. 2006; 79:271–287.

Moutoussis M, Williams J, Dayan P, Bentall RP. Persecutory delusions and the conditioned avoidance paradigm: towards an integration of the psychology and biology of paranoia. Cognitive Neuropsychiatry. 2007; 12:495–510. [PubMed: 17978936]

Ochsner KN, Gross JJ. The cognitive control of emotion. Trends Cogn Sci. 2005; 9:242–249. [PubMed: 15866151]

Olsson A, Phelps EA. Social learning of fear. Nature Neuroscience. 2007; 10:1095–1102. [PubMed: 17726475]

Ongur D, Ferry AT, Price JL. Architectonic subdivision of the human orbital and medial prefrontal cortex. Journal of Comprehensive Neurology. 2003; 460:425–449.

Ongur D, Price JL. The organization of networks within the orbital and medial prefrontal cortex of rats, monkeys and humans. Cerebral Cortex. 2000; 10:206–219. [PubMed: 10731217]

Palaniyappan L, Liddle PF. Does the salience network play a cardinal role in psychosis? An emerging hypothesis of insular dysfunction. Journal of Psychiatry & Neuroscience. 2012; 37:17–27. [PubMed: 21693094]

Pascual B, Masdeu JC, Hollenbeck M, Makris N, Insausti R, Ding SL, Dickerson BC. Large-scale brain networks of the human left temporal pole: a functional connectivity mri study. Cerebral Cortex. 2015; 25(3):680–702. [PubMed: 24068551]

Pauly KD, Kircher TT, Schneider F, Habel U. Me, myself and I: temporal dysfunctions during self-evaluation in patients with schizophrenia. Social Cognitive and Affective Neuroscience. 2013; 9:1779–1788. [PubMed: 24369435]

Phelps EA, O'Connor KJ, Gatenby JC, Gore JC, Grillon C, Davis M. Activation of the left amygdala to a cognitive representation of fear. Nature Neuroscience. 2001; 4:437–441. [PubMed: 11276236]

Phillips ML, Ladouceur CD, Drevets WC. A neural model of voluntary and automatic emotion regulation: implications for understanding the pathophysiology and neurodevelopment of bipolar disorder. Molecular Psychiatry. 2008; 13829:833–857.

Phillips ML, Williams L, Senior C, Bullmore ET, Brammer MJ, Andrew C, Williams SC, David AS. A differential neural response to threatening and non-threatening negative facial expressions in paranoid and non-paranoid schizophrenics. Psychiatry Research: Neuroimaging. 1999; 92:11–31. [PubMed: 10688157]

Pinheiro AP, McCarley RW, Thompson E, Goncalves OF, Niznikiewicz M. From semantics to feelings: how do individuals with schizophrenia rate the emotional valence of words? Schizophrenia Research and Treatment. 2012; 2012:431823. [PubMed: 22966437]

Pinkham AE, Hopfinger JB, Ruparel K, Penn DL. An investigation of the relationship between activation of a social cognitive neural network and social functioning. Schizophrenia Bulletin. 2008; 34:688–697. [PubMed: 18477583]

Pollak DD, Monje FJ, Zuckerman L, Denny CA, Drew MR, Kandel ER. An animal model of a behavioral intervention for depression. Neuron. 2008; 60:149–161. [PubMed: 18940595]

Price JL, Drevets WC. Neurocircuitry of mood disorders. Neuropsychopharmacology. 2010; 35:192–216. [PubMed: 19693001]

Protopopescu X, Pan H, Altemus M, Tuescher O, Polanecsky M, McEwen B, Silbersweig D, Stern E. Orbitofrontal cortex activity related to emotional processing changes across the menstrual cycle. Proceedings of the National Academy of Sciences of the United States of America. 2005a; 102:16060–16065. [PubMed: 16247013]

Protopopescu X, Pan H, Tuescher O, Cloitre M, Goldstein M, Engelien W, Epstein J, Yang Y, Gorman J, LeDoux J, Silbersweig D, Stern E. Differential time courses and specificity of amygdala activity in posttraumatic stress disorder subjects and normal control subjects. Biological Psychiatry. 2005b; 57:464–473. [PubMed: 15737660]

Raij TT, Valkonen-Korhonen M, Holi M, Therman S, Lehtonen J, Hari R. Reality of auditory verbal hallucinations. Brain. 2009; 132:2994–3001. [PubMed: 19620178]

Rogan MT, Leon KS, Perez DL, Kandel ER. Distinct neural signatures for safety and danger in the amygdala and striatum of the mouse. Neuron. 2005; 46:309–320. [PubMed: 15848808]

Rolls ET, Baylis LL. Gustatory, olfactory, and visual convergence within the primate orbitofrontal cortex. Journal of Neuroscience. 1994; 14:5437–5452. [PubMed: 8083747]

Russell TA, Reynaud E, Kucharska-Pietura K, Ecker C, Benson PJ, Zelaya F, Giampietro V, Brammer M, David A, Phillips ML. Neural responses to dynamic expressions of fear in schizophrenia. Neuropsychologia. 2007; 45:107–123. [PubMed: 16814818]

Sabatinelli D, Bradley MM, Fitzsimmons JR, Lang PJ. Parallel amygdala and inferotemporal activation reflect emotional intensity and fear relevance. Neuroimage. 2005; 24:1265–1270. [PubMed: 15670706]

Sabatinelli D, Lang PJ, Bradley MM, Costa VD, Keil A. The timing of emotional discrimination in human amygdala and ventral visual cortex. Journal of Neuroscience. 2009; 29:14864–14868. [PubMed: 19940182]

Schmahmann JD, Sherman JC. The cerebellar cognitive affective syndrome. Brain. 1998; 121(Pt 4): 561–579. [PubMed: 9577385]

Seymour K, Stein T, Sanders LL, Guggenmos M, Theophil I, Sterzer P. Altered contextual modulation of primary visual cortex responses in schizophrenia. Neuropsychopharmacology. 2013; 38:2607–2612. [PubMed: 23842600]

Silbersweig D, Clarkin JF, Goldstein M, Kernberg OF, Tuescher O, Levy KN, Brendel G, Pan H, Beutel M, Pavony MT, Epstein J, Lenzenweger MF, Thomas KM, Posner MI, Stern E. Failure of frontolimbic inhibitory function in the context of negative emotion in borderline personality disorder. American Journal of Psychiatry. 2007; 164:1832–1841. [PubMed: 18056238]

Silbersweig D, Stern E. Functional neuroimaging of hallucinations in schizophrenia: toward an integration of bottom-up and top-down approaches. Molecular Psychiatry. 1996; 1:367–375. [PubMed: 9154229]

Silbersweig DA, Stern E, Frith C, Cahill C, Holmes A, Grootoonk S, Seaward J, McKenna P, Chua SE, Schnorr L, et al. A functional neuroanatomy of hallucinations in schizophrenia. Nature. 1995; 378:176–179. [PubMed: 7477318]

Sommer IE, Ramsey NF, Mandl RC, Kahn RS. Language lateralization in female patients with schizophrenia: an fMRI study. Schizophrenia Research. 2003; 60:183–190. [PubMed: 12591582]

Swanson JW, Swartz MS, Van Dorn RA, Elbogen EB, Wagner HR, Rosenheck RA, Stroup TS, McEvoy JP, Lieberman JA. A national study of violent behavior in persons with schizophrenia. Archives of General Psychiatry. 2006; 63:490–499. [PubMed: 16651506]

Tandon R, Nasrallah HA, Keshavan MS. Schizophrenia, "just the facts" 4. Clinical features and conceptualization. Schizophrenia Research. 2009; 110:1–23. [PubMed: 19328655]

Taylor SF, Kang J, Brege IS, Tso IF, Hosanagar A, Johnson TD. Meta-analysis of functional neuroimaging studies of emotion perception and experience in schizophrenia. Biological Psychiatry. 2012; 71:136–145. [PubMed: 21993193]

Taylor SF, Liberzon I, Koeppe RA. The effect of graded aversive stimuli on limbic and visual activation. Neuropsychologia. 2000; 38:1415–1425. [PubMed: 10869585]

Taylor SF, Phan KL, Britton JC, Liberzon I. Neural response to emotional salience in schizophrenia. Neuropsychopharmacology. 2005; 30:984–995. [PubMed: 15689961]

Tuescher O, Protopopescu X, Pan H, Cloitre M, Butler T, Goldstein M, Root JC, Engelien A, Furman D, Silverman M, Yang Y, Gorman J, LeDoux J, Silbersweig D, Stern E. Differential activity of subgenual cingulate and brainstem in panic disorder and PTSD. Journal of Anxiety Disorders. 2011; 25:251–257. [PubMed: 21075593]

Williams LM, Das P, Harris AW, Liddell BB, Brammer MJ, Olivieri G, Skerrett D, Phillips ML, David AS, Peduto A, Gordon E. Dysregulation of arousal and amygdala-prefrontal systems in paranoid schizophrenia. American Journal of Psychiatry. 2004; 161:480–489. [PubMed: 14992974]

Williams LM, Das P, Liddell BJ, Olivieri G, Peduto AS, David AS, Gordon E, Harris AW. Fronto-limbic and autonomic disjunctions to negative emotion distinguish schizophrenia subtypes. Psychiatry Research: Neuroimaging. 2007; 155:29–44. [PubMed: 17398080]

Wolf C, Linden S, Jackson MC, Healy D, Baird A, Linden DE, Thome J. Brain activity supporting working memory accuracy in patients with paranoid schizophrenia: a functional magnetic resonance imaging study. Neuropsychobiology. 2011; 64:93–101. [PubMed: 21701227]

Worsley KJ, Liao CH, Aston J, Petre V, Duncan GH, Morales F, Evans AC. A general statistical analysis for fMRI data. Neuroimage. 2002; 15:1–15. [PubMed: 11771969]

Zhou Y, Shu N, Liu Y, Song M, Hao Y, Liu H, Yu C, Liu Z, Jiang T. Altered resting-state functional connectivity and anatomical connectivity of hippocampus in schizophrenia. Schizophrenia Research. 2008; 100:120–132. [PubMed: 18234476]

Highlights

Paranoid delusions positively correlated with fear related sensory processing

Paranoid delusions negatively correlated with safety related sensory processing

The salience network showed divergent fear and safety cued activations

Paranoid delusions positively correlated with hippocampal activations

Paranoid delusions correlated with threat word linked language network activations
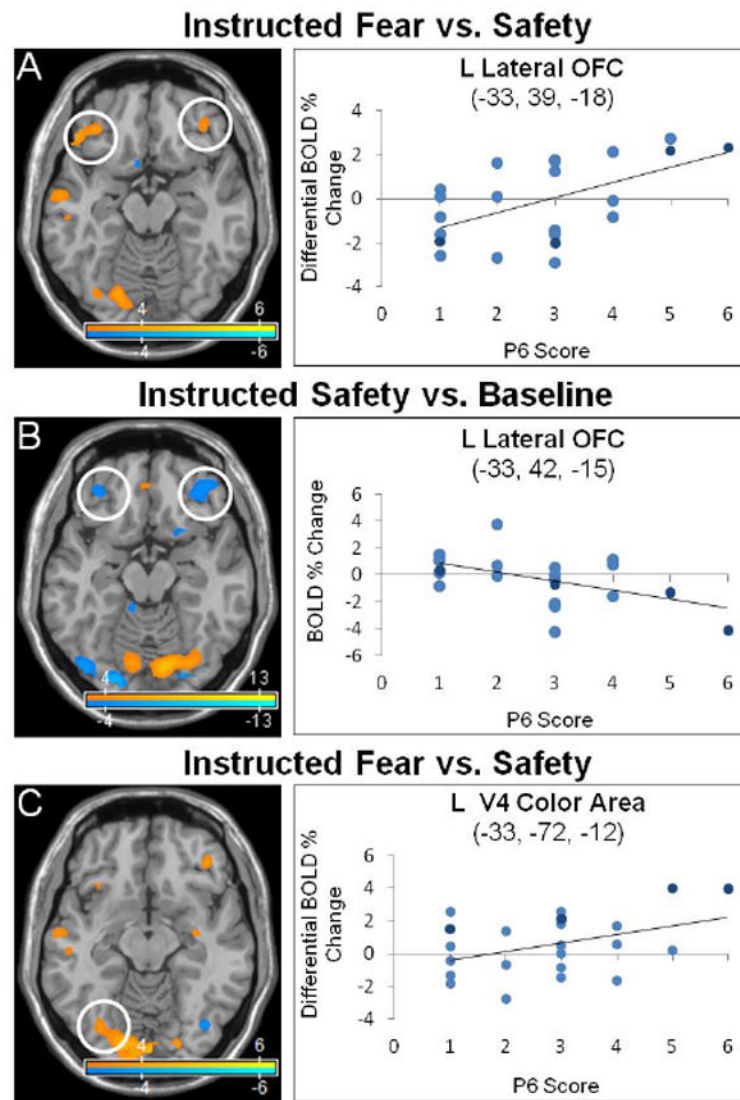
Fig. 1.
Lateral orbitofrontal cortex and V4 color area activations correlated to persecutory delusion severity in the instructed-fear/safety paradigm. Neural activations correlated with persecutory delusion severity (P6 score) were studied in patients with schizophrenia using an instructed-fear/safety paradigm. Fear and safety cues were distinguished by delivery of different colored squares. Statistical parametric maps show blood-oxygen-level-dependent (BOLD) neural activation changes thresholded at a voxelwise p-value of 0.001 for visualization purposes. **(A)** A positive correlation was observed between P6 scores and left (-33, 39, -18: peak z-score = 4.545, corrected p-value = 0.002) and right (42, 39, -12: peak z-score = 3.836, corrected p-value = 0.029) lateral orbitofrontal cortex (OFC) in the instructed-fear vs. safety contrast. **(B)** A negative correlation was observed between P6 scores and left (-33, 42, -15: peak z-score = 4.035, corrected p-value = 0.015) and right (39, 45, -12: peak z-score = 4.587, corrected p-value = 0.002) lateral OFC activations in the instructed-safety vs. baseline contrast. **(C)** Left V4 color area activation correlated with P6 scores in the

instructed-fear vs. safety contrast (-33, -72, -12; peak z-score = 3.719, corrected p-value = 0.043), while reduced V4 color area activation correlated with P6 scores in the instructed-safety vs. baseline contrast (-24, -84, -9; peak z-score = > 8, corrected p-value < 0.001; not shown). In the scatter plots, light blue indicates schizophrenia subjects, dark blue schizoaffective subjects.
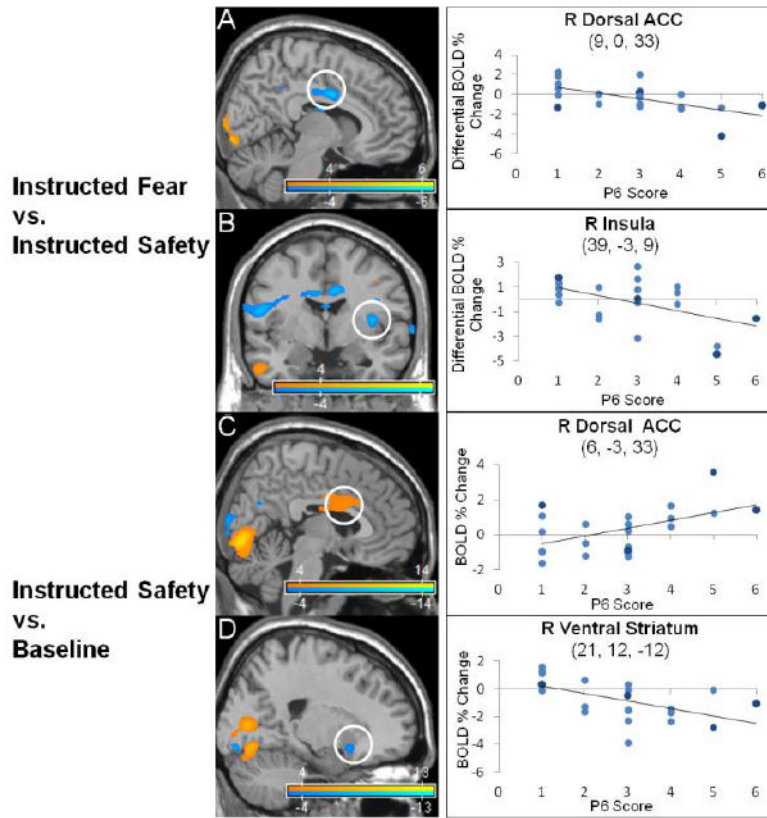
Fig. 2.
Salience network activations correlated to persecutory delusion severity in the instructed-fear/safety paradigm. Statistical parametric maps show blood-oxygen-level-dependent (BOLD) neural activation changes thresholded at a voxelwise p-value of 0.001 for visualization purposes. **(A-B)** In the instructed-fear vs. safety contrast, decreased activations in the right posterior-dorsal anterior cingulate cortex (ACC) (9, 0, 33: peak z-score = 4.923, corrected p-value < 0.001) and insula (39, -3, 9: peak z-score = 4.668, corrected p-value = 0.001) correlated with P6 scores (persecutory delusion severity). **(C-D)** In the instructed-safety vs. baseline contrast, P6 scores correlated positively with increased activations in the right posterior-dorsal ACC (6, -3, 33: peak z-score = 4.052, corrected p-value = 0.014) and insula (39, 24, 6: peak z-score = 3.996, corrected p-value = 0.017; not shown), and correlated negatively with decreased right ventral striatum (21, 12, -12: peak z-score = 4.325, corrected p-value = 0.005) activations. In the scatter plots, light blue indicates schizophrenia subjects, dark blue schizoaffective subjects.
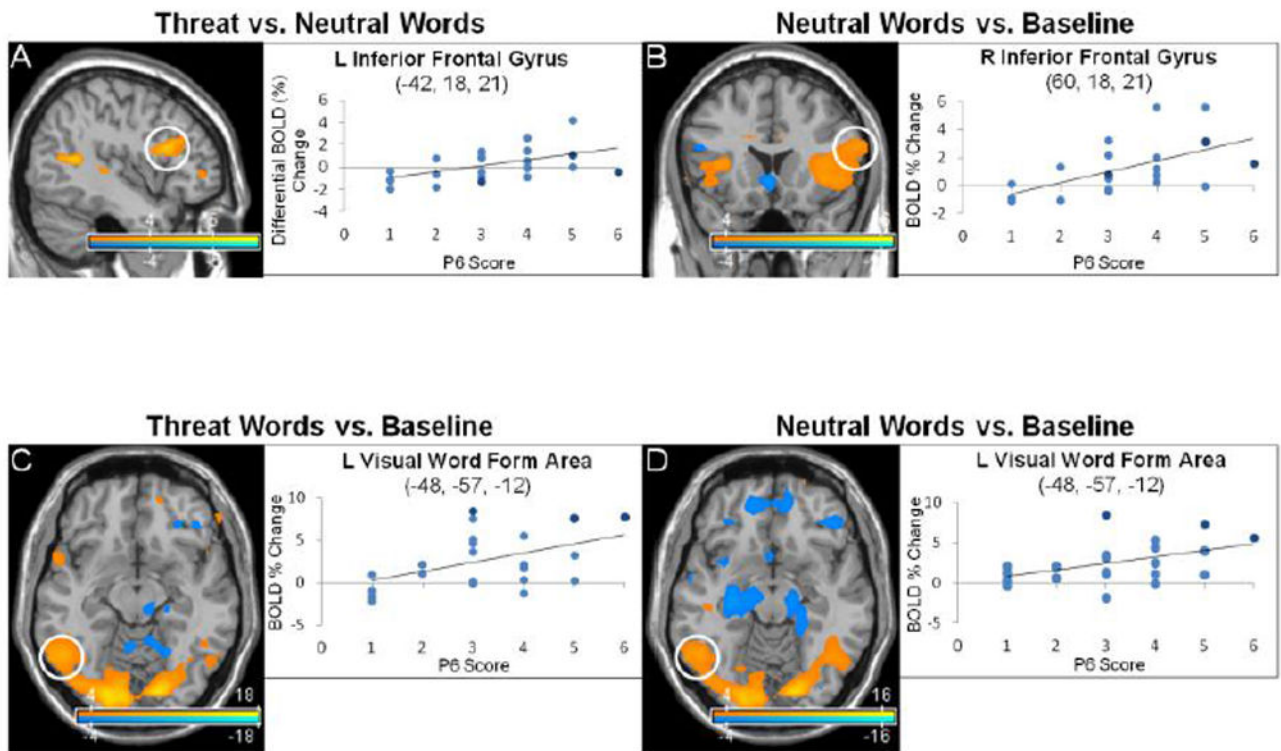
Fig. 3.

Anterior language network and visual word form area activations correlated to persecutory delusion severity in the emotional word paradigm. Statistical parametric maps show blood-oxygen-level-dependent (BOLD) neural activation changes thresholded at a voxelwise p-value of 0.001 for visualization purposes. **(A)** P6 scores (persecutory delusion severity) positively correlated with left inferior frontal gyrus, pars opercularis/triangularis (-42, 18, 21: peak z-score = 4.543, corrected p-value = 0.002) activations in the threat word vs. neutral word contrast. **(B)** P6 scores correlated positively with right (60, 18, 21: peak z-score = 5.934, corrected p-value < 0.001) and left (-48, 9, 9: peak z-score = 5.257, corrected p-value < 0.001; not shown) inferior frontal gyri for the neutral word vs. baseline contrast. **(C-D)** Visual word form area (-48, -57, -12) activations positively correlated with P6 scores in both the threat word (peak z-score > 8, corrected p-value < 0.001) and neutral word vs. baseline contrasts (peak z-score = 6.672, corrected p-value < 0.001). In the scatter plots, light blue indicates schizophrenia subjects, dark blue schizoaffective subjects.

Threat vs. Neutral Words
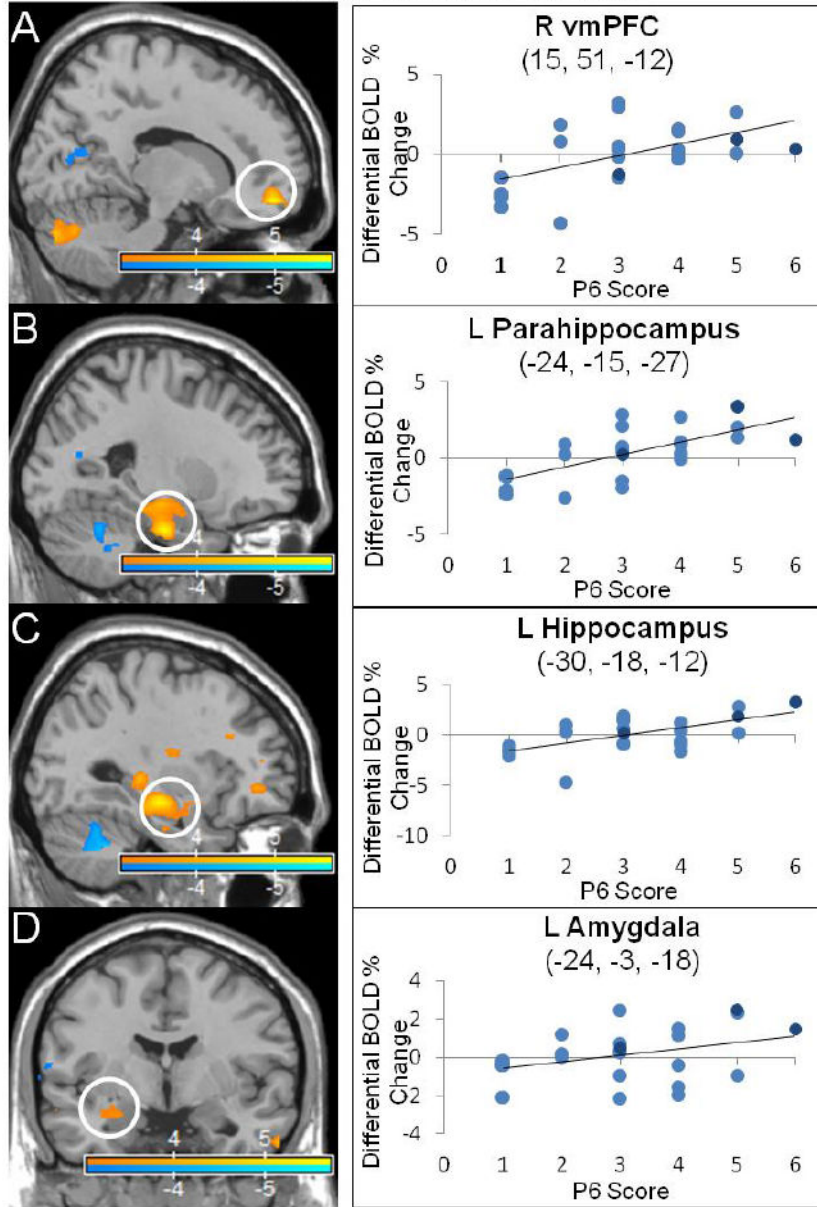
Fig. 4.
Frontolimbic activations correlated to persecutory delusion severity in the threat word versus neutral word contrast. The statistical parametric maps show blood-oxygen-level-dependent (BOLD) neural activation changes thresholded at a voxelwise p-value of 0.001 for visualization purposes. Positive correlations noted between P6 scores and **(A)** right ventromedial prefrontal cortex (vmPFC) (15, 51, -12: peak z-score = 5.653, corrected p-value < 0.001), **(B)** left parahippocampus (-24, -15, -27, peak z-score = 5.7, corrected p-value < 0.001), **(C)** left hippocampus (-30, -18, -12: peak z-score = 5.541, corrected p-value < 0.001), and **(D)** left amygdala (-24, -3, -18: peak z-score = 3.452, corrected p-value =

0.095 (trend)). In the scatter plots, light blue indicates schizophrenia subjects, dark blue schizoaffective subjects.

Table 1

Instructed-fear/safety paradigm

Brain region	Brodmann area	Peak coordinate in MNI space (mm)			Peak Z	p-corrected (whole brain)	Cluster size (mm³)
		x	y	z			
Instructed fear vs. Instructed safety							
Increase activations							
L Lingual gyrus/calcarine cortex	18	-18	-84	-9	5.901	<0.001	25893
R Calcarine cortex	17	12	-93	6	4.229	0.007	
R Lingual gyrus	17	9	-90	-6	4.975	<0.001	
L Fusiform gyrus, posterior	19	-36	-75	-18	3.943	0.02	
L Fusiform gyrus (V4, color area)	19	-33	-72	-12	3.719	0.043	
L Inferior frontal gyrus (orbitalis)/orbitofrontal cortex, lateral	47	-33	39	-18	4.545	0.002	2943
R Orbitofrontal cortex, lateral/inferior frontal gyrus (orbitalis)	47	42	39	-12	3.836	0.029	3591
R Orbitofrontal cortex, posterior-lateral	47	33	-9	-9	3.746	0.039	891
L Frontopolar cortex	10	-21	57	12	3.955	0.02	1620
L Middle temporal gyrus	21	-54	6	-30	4.644	0.001	8694
R Middle temporal gyrus	37	63	-60	0	3.736	0.041	2160
R Temporal pole	38	39	9	-24	3.679	0.048	837
Decrease activations							
R Supramarginal gyrus	40	42	-30	45	6.237	<0.001	72954
R Postcentral gyrus	3	45	-27	42	5.721	<0.001	
L Postcentral gyrus		-51	-3	18	4.751	0.001	
R Precentral gyrus	6	54	3	21	3.984	0.018	
R Posterior-dorsal anterior cingulated cortex/middle cingulate cortex		9	0	33	4.923	<0.001	
L Posterior-dorsal anterior cingulated cortex/middle cingulate cortex		-6	0	33	4.884	<0.001	
R Insula, anterior		39	6	18	4.309	0.005	
R Insula, middle-posterior		39	-3	9	4.668	0.001	
R Inferior frontal gyrus, opercularis	44	57	12	24	4.152	0.01	
R Superior occipital gyrus	7	33	-69	45	4.102	0.012	
R Angular gyrus	40	36	-54	42	4.033	0.015	

Brain region	Brodmann area	Peak coordinate in MNI space (mm)			Peak Z	p-corrected (whole brain)	Cluster size (mm³)
		x	y	z			
R Precuneus		6	-48	39	3.812	0.032	
R Superior temporal gyrus	22	69	-9	3	4.019	0.016	
L Middle occipital gyrus/superior occipital gyrus	7	-24	-63	36	4.415	0.004	3321
R Inferior occipital gyrus	19	39	-72	-12	3.806	0.032	756
L Inferior frontal gyrus, triangularis	45	-42	24	12	3.725	0.042	567
Instructed fear vs. baseline							
Increase activations							
L Calcarine cortex/lingual gyrus	17	-6	-84	0	>8	<0.001	53838
R Calcarine cortex	18	18	-78	6	>8	<0.001	
R Lingual gyrus	18/17	6	-84	-9	>8	<0.001	
L Fusiform gyrus, posterior	19	-30	-75	-18	7.273	<0.001	
L Fusiform gyrus	37	-36	-54	-21	5.447	<0.001	
R Fusiform gyrus	37	33	-54	-15	4.525	0.002	
R Inferior frontal gyrus, orbitalis	38	48	21	-9	4.865	0.001	8586
R Inferior frontal gyrus, triangularis	45	45	27	6	4.703	0.001	
R Insula, anterior	47	45	21	-6	4.484	0.003	
L Inferior frontal gyrus, triangularis	47	-45	30	0	4.796	0.001	7479
L Orbitofrontal cortex, posterior-lateral/inferior frontal gyrus, orbitalis	47	-33	24	-9	4.336	0.005	
L Orbitofrontal cortex, lateral	47	-36	36	-18	4.158	0.01	
R Middle frontal gyrus	46	33	54	27	4.669	0.001	4185
R Superior frontal gyrus	46	24	48	24	4.479	0.003	
R Superior medial frontal gyrus	9	6	45	33	4.03	0.015	621
R Precentral gyrus	44	48	12	33	3.749	0.039	1242
L Inferior parietal cortex	2	-57	-27	45	3.998	0.017	729
R Temporal pole, medial	38	33	21	-27	4.314	0.005	3564
R Superior temporal gyrus/rolandic operculum		54	-21	15	4.305	0.006	2241
L Middle temporal gyrus	21	-54	3	-30	3.878	0.025	3510
L Middle temporal gyrus	21	-63	-12	-9	3.874	0.026	2538
R Middle temporal gyrus	22	57	-15	-9	3.973	0.018	4293

Brain region	Brodmann area	Peak coordinate in MNI space (mm)			Peak Z	p-corrected (whole brain)	Cluster size (mm³)
		x	y	z			
R Hippocampus, anterior	20	36	-9	-12	3.945	0.02	
Decrease activations							
L Lingual gyrus	18	-24	-87	-12	>8	<0.001	5049
L Inferior occipital gyrus	18	-24	-84	-9	>8	<0.001	
R Inferior occipital gyrus	19	39	-81	-9	7.268	<0.001	5643
R Middle temporal gyrus	37	48	-69	0	4.017	0.016	
R Middle occipital gyrus	19	36	-81	30	5.138	<0.001	5859
R Insula, middle		39	-3	12	5.776	<0.001	17982
R Postcentral gyrus	3	57	-12	36	5.379	<0.001	
R Cuneus	18	18	-93	15	4.246	0.007	783
L Precentral gyrus		-48	-3	21	4.592	0.002	7452
L Inferior parietal lobule/angular gyrus	7	-36	-72	45	4.689	0.001	5400
L Middle occipital gyrus	7	-27	-60	36	3.904	0.023	
R Posterior cingulate cortex/precuneus	31	3	-45	39	4.084	0.012	8775
R Posterior-dorsal anterior cingulated cortex/middle cingulate cortex		12	0	36	3.782	0.035	1296
L Rostral anterior cingulate cortex	11	-9	39	0	3.754	0.038	1053
R Pons, dorsal		3	-36	-42	4.676	0.001	891
L Cerebellum, 7b		-15	-69	-39	3.706	0.045	459
Instructed safety vs. baseline							
Increase activations							
L Calcarine cortex	17	-9	-84	3	>8	<0.001	30159
R Lingual gyrus	18	12	-78	-12	>8	<0.001	
R Calcarine cortex	18/17	18	-78	6	>8	<0.001	
R Fusiform gyrus	19	30	-75	-12	5.797	<0.001	
R Middle occipital gyrus	18	27	-87	3	3.911	0.023	
R Dorsal-anterior anterior cingulate cortex		9	12	27	5.201	<0.001	29835
R Posterior-dorsal anterior cingulate Cortex		6	-3	33	4.052	0.014	
L Posterior-dorsal anterior cingulate cortex	24	-6	3	33	4.027	0.015	
R Anterior insula	47	39	24	6	3.996	0.017	

Brain region	Brodmann area	Peak coordinate in MNI space (mm)			Peak Z	p-corrected (whole brain)	Cluster size (mm³)
		x	y	z			
R Inferior frontal gyrus, triangularis	45	45	27	6	3.906	0.023	
R Inferior frontal gyrus, opercularis	44	54	15	36	3.779	0.035	
L Anterior insula	47	-39	21	3	4.493	0.003	3672
L Superior occipital cortex	19	-18	-69	39	4.896	<0.001	7803
L Precuneus	7	-12	-63	45	4.141	0.01	
R Superior occipital cortex	7	33	-72	45	4.139	0.01	486
R Supramarginal gyrus	2,40	45	-33	45	5.336	<0.001	8019
L Supramarginal gyrus	40	-51	-39	33	3.826	0.03	7533
L Fusiform gyrus	37	-36	-54	-21	5.448	<0.001	2592
L Cerebellum, 6		-30	-72	-18	4.118	0.011	648
Decrease activations							
L Inferior occipital gyrus/fusiform gyrus (V4, color area)	18	-24	-84	-9	>8	<0.001	12312
L Lingual gyrus	18	-21	-87	-12	>8	<0.001	
L Fusiform gyrus	19	-42	-78	-15	5.347	<0.001	
L Middle occipital gyrus	19	-33	-81	3	5.31	<0.001	
L Calcarine cortex	18	-9	-93	-12	4.104	0.012	
R Lingual gyrus	18	24	-87	-12	>8	<0.001	4671
R Inferior occipital gyrus	19	39	-81	-9	6.474	<0.001	
R Inferior temporal gyrus, posterior portion	37	15	-69	-3	4.0464	0.013	
R Cuneus	17	12	-96	12	7.598	<0.001	4320
R Calcarine cortex	18	3	-93	9	6.126	<0.001	
R Lingual gyrus	18	18	-78	-3	3.902	0.024	135
L Middle occipital gyrus	39	-39	-78	33	3.896	0.024	3402
R Orbitofrontal cortex, lateral	47	39	45	-12	4.587	0.002	2538
R Ventral striatum		21	12	-12	4.325	0.005	2673
L Orbitofrontal cortex, lateral	47/11	-33	42	-15	4.035	0.015	2241
L Superior frontal gyrus	9	-12	51	39	4.04	0.015	1377
R Cuneus		0	-66	27	3.897	0.024	918
L Precentral gyrus	6	-42	9	42	4.06	0.014	864

Brain region	Brodmann area	Peak coordinate in MNI space (mm)			Peak Z	p-corrected (whole brain)	Cluster size (mm³)
		x	y	z			
R Inferior temporal gyrus	37	60	-57	-12	3.91	0.023	756

Note: Brain regions showing differential blood-oxygen-level-dependent (BOLD) neural activations in schizophrenic patients correlated to persecutory delusion severity (P6 scores) for the contrasts (1) instructed-fear vs. safety, (2) instructed-fear vs. baseline, and (3) instructed-safety vs. baseline as also shown in Fig. 1 and Fig. 2. Cluster sizes are reported at a voxel-wise $p<0.01$, and all voxel-wise p-values are less than 0.0001 at the listed peak coordinates. L, left;

Emotional word paradigm

Table 2

Brain region	Brodmann area	Peak coordinate in MNI space (mm)			Peak Z	*p*-corrected (whole brain)	Cluster size (mm³)
		x	*y*	*z*			
Threat words vs. neutral words							
Increase activations							
R Ventromedial prefrontal cortex	11	15	51	-12	5.653	<0.001	18090
L Ventromedial prefrontal cortex	11	-15	42	-12	4.171	0.009	
L Inferior frontal gyrus (orbitalis)	47	-33	42	-3	4.847	0.001	
L Middle orbitofrontal/middle frontal gyrus	47	-36	45	0	4.93	<0.001	
L Frontopolar cortex	10	-3	60	21	4.192	0.008	
R Frontopolar cortex	10	0	63	0	3.755	0.038	
L Parahippocampal gyrus	36	-24	-15	-27	5.7	<0.001	16659
L Hippocampus	20	-30	-18	-12	5.541	<0.001	
L Amygdala	*34*	*-24*	*-3*	*-18*	*3.452*	*0.095*	
L Midbrain		-6	-18	-18	4.086	0.012	
L Insula, ventral	13	-33	3	-12	3.918	0.022	
L Superior temporal gyrus	38	-51	6	-12	4.147	0.01	
L Superior temporal gyrus, posterior	21	-45	-27	3	3.869	0.026	
L Inferior frontal gyrus, opercularis/triangularis		-42	18	21	4.543	0.002	6804
L Middle temporal gyrus	21	-42	-51	12	4.847	0.001	2862
R Middle temporal gyrus		66	-54	-9	3.82	0.031	378
R Inferior temporal gyrus	20	60	-3	-33	4.194	0.008	1377
R Fusiform gyrus	20	39	-18	-27	3.97	0.019	432
L Insula, middle		-30	-9	18	3.715	0.043	1269
R Cerebellum, 2		12	-81	-30	4.493	0.003	7182
R Cerebellum, 1		18	-78	-30	4.121	0.011	
R Cerebellum, 6		15	-69	-27	4.073	0.013	
Decrease activations							
L Cuneus		-6,	-72	27	4.43	0.003	8046

Brain region	Brodmann area	x	y	z	Peak Z	p-corrected (whole brain)	Cluster size (mm³)
L Calcarine cortex		-3	-69	24	3.782	0.035	
R Superior temporal gyrus/middle temporal gyrus	42/22	48	-18	-6	4.154	0.01	4806
R Superior frontal gyrus/middle frontal gyrus	46	30	57	18	4.081	0.013	3294
R Angular gyrus/superior temporal gyrus (posterior)/temporoparietal junction	22/42	48	-48	24	4.271	0.006	5373
R Supramarginal gyrus		57	-39	27	3.73	0.041	
R Middle temporal gyrus	22	54	-48	21	4.044	0.014	
L Middle temporal gyrus/superior temporal gyrus, posterior	21/22	-69	-24	6	4.877	0.001	2673
R Inferior frontal gyrus, opercularis/anterior insula	47	48	18	0	3.691	0.047	3159
R Inferior lateral orbitofrontal cortex	38	39	30	-24	4.082	0.013	1431
L Operculum, rolandic	6	-63	3	12	4.224	0.007	2241
L Superior orbitofrontal cortex	11	-18	66	-3	3.883	0.025	513
R Cerebellar vermis 4, 5		6	-57	15	3.823	0.031	2295
R Cerebellum, 6		30	-51	-27	4.031	0.015	1755
R Pons, dorsal		9	-36	33	5.083	<0.001	8910
L Cerebellum, 8, 7b, 6		-30	-54	-39	4.563	0.002	
Threat words vs. baseline							
Increase activations							
L Calcarine cortex	17	-9	-87	3	>8	<0.001	180252
R Lingual gyrus	18	15	-87	-9	>8	<0.001	
L Middle occipital gyrus	18	-27	-84	3	>8	<0.001	
R Middle occipital gyrus	18	30	-84	6	>8	<0.001	
R Cuneus	18	21	-87	15	>8	<0.001	
L Cuneus	18	-9	-90,	24	6.428	<0.001	
L Fusiform gyrus	19	-39	-78	-12	7.233	<0.001	
R Fusiform gyrus	37	36	-39	-21	6.105	<0.001	
L Inferior temporal gyrus	37	-57	-60	-9	>8	<0.001	
L Inferior temporal gyrus/visual word form area	37	-48	-57	-12	>8	<0.001	
R Inferior temporal gyrus	37	60	-60	-6	5.891	<0.001	
L Inferior occipital gyrus	19	-39	-72	-3	6.252	<0.001	

Brain region	Brodmann area	Peak coordinate in MNI space (mm)			Peak Z	p-corrected (whole brain)	Cluster size (mm³)
		x	y	z			
L Superior occipital gyrus	18	-15	-87	27	5.647	<0.001	
L Inferior frontal gyrus, triangularis	45,47	-39	24	9	7.942	<0.001	
L Inferior frontal gyrus, opercularis	44	-45	9	15	6.738	<0.001	
L Opercular rolandic		-42	0	18	5.91	<0.001	
R Opercular rolandic	22	66	-18	18	5.345	<0.001	
R Inferior frontal gyrus, opercularis	44	66	15	21	7.51	<0.001	
R Inferior frontal gyrus, triangularis	47	60	36	9	5.229	<0.001	
R Inferior frontal gyrus, orbitalis	38	57	24	-6	4.656	0.001	
L Middle frontal gyrus	46	-24	39	24	5.432	<0.001	
L Middle temporal gyrus	22	-45	-51	9	5.069	<0.001	
R Middle temporal gyrus	21	60	-51	0	4.091	0.012	
L Superior temporal gyrus	42	-57	-30	21	6.023	<0.001	
L Temporal pole, superior	38	-54	9	-9	5.154	<0.001	
R Temporal pole, superior	38	51	15	-15	4.229	0.007	
R Heschl's gyrus		45	-15	9	4.019	0.016	
R Supramarginal gyrus/superior temporal gyrus, posterior		60	-27	24	6.02	<0.001	
L Middle temporal gyrus	21	-60	-27	3	4.531	0.002	
L Insula, anterior	47	-33	24	-3	5.644	<0.001	
L Insula, middle		-39	6	0	5.129	<0.001	
R Insula, anterior	47	33	27	3	5.506	<0.001	
L Anterior-dorsal anterior cingulate cortex		-12	30	18	3.691	0.046	
L Cerebellum, 6		-15	-69	-21	5.561	<0.001	
R Middle frontal gyrus	46	33	45	21	3.984	0.018	1107
L Parahippocampal gyrus	36	-27	-15	-27	3.662	0.051	1728
R Fusiform gyrus	20	39	-18	-27	4.602	0.002	1053
R Parahippocampal gyrus	35	21	-15	-24	3.607	0.06	891
R Anterior-dorsal anterior cingulate cortex	24	9	18	27	4.921	<0.001	783
L Middle orbitofrontal cortex	11	-27	54	-15	3.813	0.032	270
R Superior orbitofrontal cortex	11	18	54	-15	3.935	0.021	324

Brain region	Brodmann area	Peak coordinate in MNI space (mm)			Peak Z	p-corrected (whole brain)	Cluster size (mm³)
		x	y	z			
Decrease activations							
R Lingual gyrus	17	9	-57	9	7.182	<0.001	74439
R Lingual gyrus	19	21	-57	0	4.449	0.003	
R Calcarine cortex	17	12	-60	12	6.76	<0.001	
L Calcarine cortex	17	-12	-57	9	6.425	<0.001	
R Precuneus	23	3	-63	24	6.353	<0.001	
L Precuneus	29	-9	-48	9	4.732	0.001	
L Cuneus	23	-3	-66	24	6.43	<0.001	
R Cuneus	23	6	-60	21	6.254	<0.001	
L Fusiform gyrus, anterior	37	-24	-36	-21	4.554	0.002	
R Middle temporal gyrus	39	45	-51	21	3.862	0.027	
R Supramarginal gyrus/superior temporal gyrus, posterior/temporal parietal junction	40, 22	60	-48	24	5.811	<0.001	
R Angular gyrus	39	42	-57	27	4.51	0.002	
R Thalamus, posterior medial		9	-27	6	5.758	<0.001	
L Thalamus, dorsomedial		-6	-15	15	3.947	0.02	
L Cerebellum, 6		-39	-63	-21	5.213	<0.001	
R Cerebellum, 6		30	-54	-24	3.904	0.023	
R Cerebellum, 4, 5		15	-48	-9	4.514	0.002	
L Cerebellum, 8		-12	-60	-39	4.383	0.004	
R Cerebellar vermis		6	-69	-39	3.938	0.021	
R Pons, dorsal		6	-27	-15	4.288	0.006	
R Rostral anterior cingulate cortex	32	12	36	9	4.681	0.001	17550
R Subgenual anterior cingulate cortex	25	3	18	-6	3.741	0.04	
R Rostral anterior cingulate cortex	32	12	45	6	3.651	0.053	
L Frontopolar cortex	10,11	-12	63	-3	3.965	0.019	
R Caudate, head		12	9	3	3.983	0.018	
R Thalamus, posterior medial		9	-27	6	5.758	<0.001	
R Inferior occipital cortex	18	24	-96	0	7.09	<0.001	270
L Angular gyrus	39	-45	-72	27	5.301	<0.001	2700

Brain region	Brodmann area	Peak coordinate in MNI space (mm)			Peak Z	p-corrected (whole brain)	Cluster size (mm³)
		x	y	z			
R Temporal pole, medial	38	36	21	-33	5.466	<0.001	6858
R Middle-posterior orbitofrontal cortex	47,11	33	39	-18	5.014	<0.001	
L Temporal pole, superior	38	-45	24	-24	4.679	0.001	2133
R Frontopolar cortex	10	6	66	24	4.974	<0.001	1269
R Superior temporal gyrus	22	60	-9	0	4.938	<0.001	1053
L Opercular, rolandic		-60	-3	12	4.371	0.004	2511
R Inferior frontal gyrus, triangularis		39	24	27	4.392	0.004	1647
L Posterior cingulate cortex	23	-6	-36	27	3.83	0.03	513
R Cerebellum, 1		42	-69	-21	4.488	0.003	1377
Neutral words vs. baseline							
Increase activations							
L Calcarine cortex	17	-9	-87	3	>8	<0.001	89424
R Calcarine cortex	18/17	18	-90	3	>8	<0.001	
R Superior occipital gyrus	19	27	-72	24	6.179	<0.001	
L Superior occipital gyrus/cuneus	18	-12	-90	24	4.297	0.006	
R Cuneus	18	18	-87	12	7.707	<0.001	
L Middle occipital gyrus	18	-27	-87	6	>8	<0.001	
R Middle occipital gyrus	18	36	-84	6	8.014	<0.001	
L Inferior occipital gyrus	19	-45	-72	-12	5.197	<0.001	
L Lingual gyrus	18	-21	-87	-12	>8	<0.001	
R Lingual gyrus	18	15	-87	-9	>8	<0.001	
R Superior temporal gyrus	21/22	57	-21	-3	5.584	<0.001	
L Middle temporal gyrus	37	-45	-51	-3	6.303	<0.001	
R Middle temporal gyrus	21	57	-51	0	6.191	<0.001	
L Inferior temporal gyrus	37	-51	-57	-9	7.058	<0.001	
L Inferior temporal gyrus/visual word form area	37	-48	-57	-12	6.672	<0.001	
R Inferior temporal gyrus	37	51	-60	-9	5.261	<0.001	
L Fusiform gyrus	19	-39	-78	-12	5.882	<0.001	
R Fusiform gyrus	37	33	-36	-21	5.703	<0.001	

Brain region	Brodmann area	Peak coordinate in MNI space (mm)			Peak Z	p-corrected (whole brain)	Cluster size (mm³)
		x	y	z			
L Cerebellum, 6		-18	-66	-18	5.543	<0.001	36180
R Cerebellum, 6, 5, 4		18	-51	-24	4.273	0.006	
R Anterior insula	47	39	21	-3	7.189	<0.001	
R Inferior frontal gyrus, opercularis	44	60	18	21	5.934	<0.001	
R Inferior frontal gyrus, orbitalis	47	48	21	-6	5.649	<0.001	
R Inferior frontal gyrus, triangularis	45	45	30	3	5.18	<0.001	
R Middle frontal gyrus	46	36	54	21	4.585	0.002	
R Superior frontal gyrus	46	21	51	24	3.86	0.027	
R Superior frontal gyrus	9	18	54	27	3.74	0.04	
L Anterior insula		-33	24	9	7.942	<0.001	19116
L Inferior frontal gyrus, triangularis	44	-42	12	27	5.336	<0.001	
L Inferior frontal gyrus, opercularis		-48	9	9	5.257	<0.001	
L Inferior frontal gyrus, orbitalis	47	-42	21	-6	4.667	0.001	
L Opercular rolandic		-48	-3	9	3.903	0.023	
L Temporal pole, superior	38	-54	12	-6	3.734	0.041	
L Superior temporal gyrus	42	-57	-30	18	6.781	<0.001	10017
R Supramarginal gyrus		63	-27	24	6.001	<0.001	7425
L Middle frontal gyrus	46	-27	45	21	4.942	<0.001	7479
R Cerebellum, 1		42	-51	-33	4.444	0.003	405
R Anterior-dorsal anterior cingulate cortex	24	9	18	27	3.924	0.022	351
L Middle-orbitofrontal cortex	11	-15	30	-18	4.142	0.01	216
Decrease activations							
L Precuneus	30	-6	-54	12	6.357	<0.001	97686
L Calcarine cortex	17	-12	-57	9	6.141	<0.001	
R Calcarine cortex	23	12	-54	12	3.914	0.023	
R Precuneus	30	6	-51	9	5.372	<0.001	
L Cuneus	23	-15	-60	24	4.066	0.013	
L Fusiform gyrus, anterior	37	-27	-33	-21	6.206	<0.001	
L Fusiform gyrus, posterior	37	-33	-42	-24	4.31	0.005	

Brain region	Brodmann area	Peak coordinate in MNI space (mm)			Peak Z	p-corrected (whole brain)	Cluster size (mm³)
		x	y	z			
L Hippocampus	20	-27	-18	12	6.126	<0.001	
L Parahippocampal gyrus	20	-30	-24	-15	5.388	<0.001	
R Parahippocampal gyrus	30	24	-27	-12	4.031	0.015	
R Frontopolar cortex	10	6	66	3	5.889	<0.001	
L Frontopolar cortex	10	-3	63	27	4.415	0.004	
L Ventromedial prefrontal cortex	10,11	-9	48	-9	5.347	<0.001	
R Ventromedial prefrontal cortex	10	12	48	-12	4.135	0.01	
L Subgenual anterior cingulate cortex	25	-9	24	-3	4.583	0.002	
L Posterior-medial orbitofrontal cortex	11	-12	30	-6	5.369	<0.001	
R Posterior-medial orbitofrontal cortex	11	6	30	-9	4.178	0.009	
L Midbrain		-6	-18	-18	5.129	<0.001	
R Midbrain		15	-18	-12	4.536	0.002	
R Thalamus, anterior		6	-3	0	4.257	0.007	
L Thalamus, dorsal		-12	-21	18	4.105	0.012	
L Cerebellum, 6		-36	-42	-27	4.129	0.011	
R Cerebellum, 2		12	-81	-30	5.581	<0.001	10152
R Cerebellum, 1		33	-81	-30	4.935	<0.001	
R Lingual Gyrus	18	9	-72	-6	4.89	<0.001	1296
L Inferior frontal gyrus, triangularis	45	-48	27	18	5.69	<0.001	4077
L Angular gyrus	39	-42	-57	27	4.807	0.001	2646
L Middle occipital gyrus	39	-45	-78	27	4.528	0.002	
R Inferior frontal gyrus, orbitalis	47	42	36	-12	4.669	0.001	2241
L Inferior frontal gyrus, orbitalis	47	-30	39	-6	3.857	0.027	2106
R Superior temporal gyrus	22	69	-9	3	6.106	<0.001	2160
L Cerebellum, 1		-33	-78	-30	4.871	0.001	1782
L Middle temporal gyrus	37	-48	-63	12	4.46	0.003	1404
L Middle temporal gyrus	22	-63	-48	12	4.587	0.002	999
L Middle temporal gyrus	21	-57	-3	-15	4.178	0.009	918
R Inferior temporal gyrus	21	60	-3	-33	4.184	0.009	864
R Inferior occipital gyrus	19	36	-81	-12	3.979	0.018	513

Note: Brain regions showing differential blood-oxygen-level-dependent (BOLD) neural activations in schizophrenic patients correlated to persecutory delusion severity (P6 scores) for the contrasts (1) threat words vs. neutral words, (2) threat words vs. baseline, and (3) neutral words vs. baseline as also shown in Fig. 3 and Fig. 4. Cluster sizes are reported at a voxel-wise $p<0.01$, and all voxel-wise p-values are less than 0.0001 at the listed peak coordinates. L, left; R, right.